DETERMINING THE DEFORMATION HISTORY OF A NEWLY DISCOVERED HOLOCENE FAULT IN THE WABASH VALLEY SEISMIC ZONE, WESTERN KENTUCKY:
Collaborative Research between the Kentucky Geological Survey and the University of Cincinnati

Final Technical Report

U.S. Project Period: 12/01/10 - 05/01/12

Ronald Counts, P.I.
Kentucky Geological Survey
1401 Corporate Court
Henderson, Kentucky 42420
Tel: 270.827.3414 ext. 27, Fax: 270.827.1117
E-mail: rcounts@uky.edu

and

Lewis Owen, Co-P.I.
Department of Geology
University of Cincinnati
P.O. Box 210013
Cincinnati, OH 45221-0013

E-mail: lewis.owen@uc.edu

Program Element III: Research on Earthquake Occurrence, Physics, and Effects — Central and Eastern United States

Key Words: paleoseismology, Wabash Valley seismic zone seismic reflection, luminescence dating (OSL)

Research supported by the U.S. Geological Survey (USGS), Department of the Interior, under USGS award numbers G11AP20013 and G11AP20011. The views and conclusions contained in this document are those of the authors and should not be interpreted as necessarily representing the official policies, either expressed or implied, of the U.S. Government.

DETERMINING THE DEFORMATION HISTORY OF A NEWLY DISCOVERED HOLOCENE FAULT IN THE WABASH VALLEY SEISMIC ZONE, WESTERN KENTUCKY: Collaborative Research between the Kentucky Geological Survey and the University of Cincinnati

Ronald Counts, Kentucky Geological Survey, and
Lewis Owen, Department of Geology, University of Cincinnati

Abstract

The Uniontown fault is a north-south oriented fault in the southern Wabash Valley seismic zone, located immediately east of the Hovey Lake fault system in western Kentucky. A trench excavated across the fault in 2008 exposed Holocene alluvium folded in a down-to-the-west monocline. The goal of this project was to use a multi-disciplinary approach involving sedimentology, geophysics, and optically stimulated luminescence (OSL) dating to extend the paleoseismic record of this fault. Eight sites were cored to depths ranging from 9 – 13.5 m deep along a transect parallel to the 2008 trench site. Core descriptions, magnetic susceptibility measurements, and natural downhole gamma logs produced data consistent with observations made from the trench.

Ground penetrating radar (GPR), electrical resistivity profiles (ER), and S-wave seismic reflection profiles were acquired across the Uniontown fault. The GPR profile revealed reflectors beneath the scarp offset in a way that resembled a small half-graben. Sand, clay, and the bedrock surface are clearly visible in the ER profile. The ER profile shows that both the bedrock surface and the top of the sand are offset beneath the scarp, but the offset is much greater at the bedrock surface. Whether the larger offset in the bedrock represents multiple slip events or a single event could not be determined. Two S-wave seismic reflection profiles were acquired across the northern and southern ends of the Uniontown fault. Offset reflectors were visible in in the bedrock surface in both profiles, but faults were more numerous in the southern profile and the offset was much larger.

OSL ages of deposits and landforms around the scarp cluster into four distinctive time intervals: late Pleistocene to early Holocene (15.8 –8.2 ka), early Holocene (10.1 – 5.4 ka), early to mid-Holocene (8.9 – 3.7 ka), and late Holocene (2.19 – 1.9 ka). The age of an OSL sample taken from the folded alluvium in the 2008 trench, 4.86±0.68, is consistent with the calibrated radiocarbon age of charcoal in the trench (4,088 ±57). The late Holocene deposits post-date faulting, indicating the timing of the most recent movement on the Uniontown fault was between 5.5 and 1.5 ka, which is also when the modern channel course of the Ohio River was established around the Uniontown fault. The OSL chronology identifies four phases of fluvial landform development since the late Pleistocene, and one or more of these could represent fluvial adjustments to older paleoearthquakes.

Introduction

This study examines the deformation history of a recently discovered active fault, which we call the Uniontown fault, in the Wabash Valley Siesmic Zone. The Wabash Valley Seismic Zone is a loosely defined region of active seismicity within the lower Wabash River valley in southwestern Indiana, southeastern Illinois, and western Kentucky (Nuttli et al., 1974, Nuttli 1979) (Fig. 1). This region is underlain by a deep fault system in Precambrian basement and a shallow

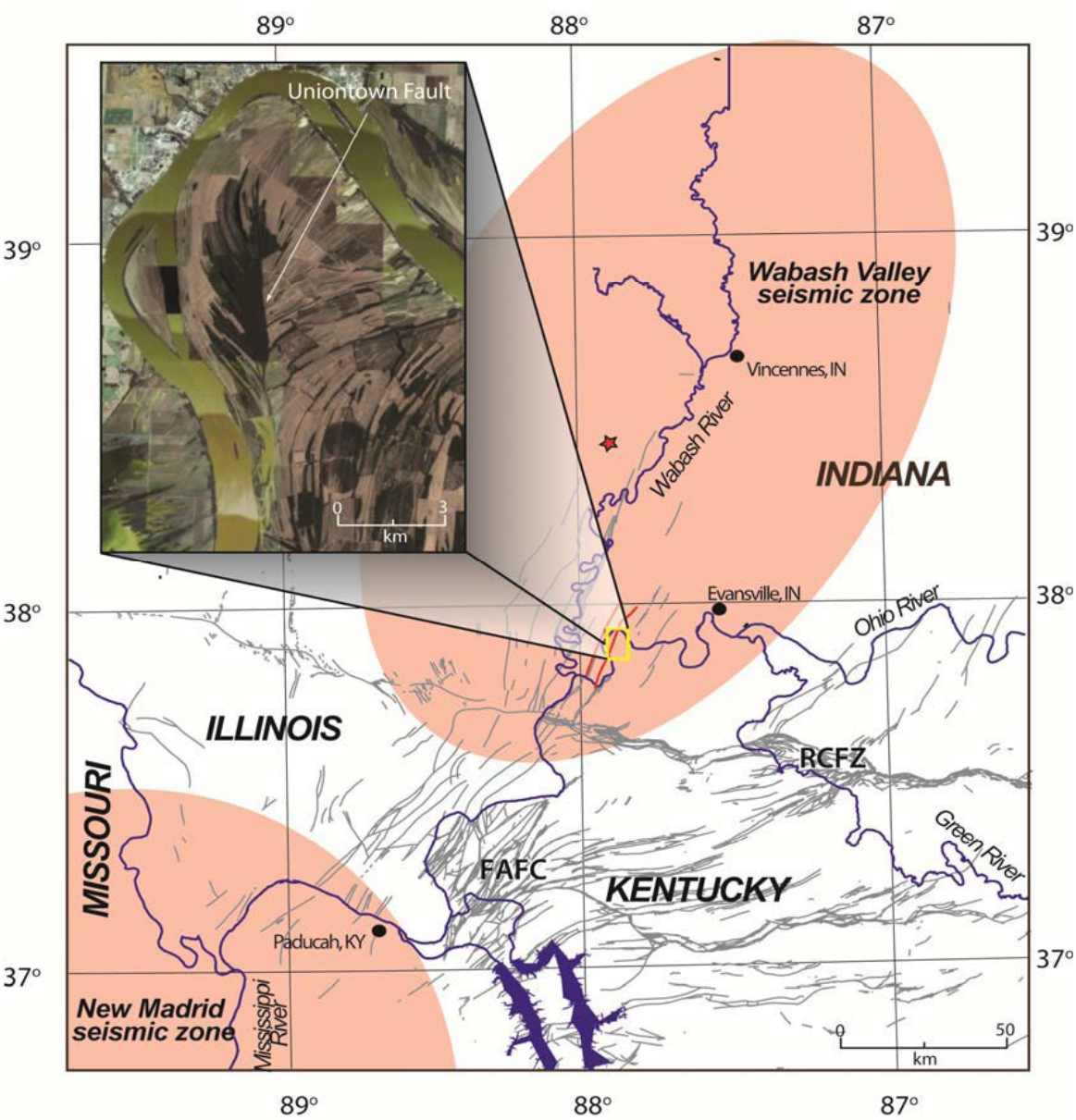

Figure 1. The Wabash Valley Seismic Zone and surrounding features. The red lines define the Hovey Lake Fault System, and the Uniontown Fault is likely part of this system. The gray lines are mapped bedrock faults: RCFZ and FAFC are the Rough Creek Fault Zone and the Fluorspar Area Fault Complex, respectively. The red star indicates the epicenter for the April 18, 2008, M 5.2 earthquake (modified from Counts et al., 2008).

fault system in overlying Paleozoic sedimentary rocks (Bristol and Treworgy, 1979). The near-surface faulting the Wabash Valley fault system and is a series of northeastern-trending, steeply-dipping high-angle normal faults (Bristol and Treworgy, 1979; Sexton et al., 1986; Nelson, 1991; Bear et al., 1997). The relationship between the deep and shallow fault systems is complex and remains unclear. Some of the near-surface faults are flower structures that merge downward into deep basement faults (Rene and Stanonis, 1995). Other near-surface faults merge downward but do not detectably offset basement strata, suggesting they were formed by post-Pennsylvanian crustal warping (Nelson, 1991). Some researchers have inferred from seismic reflection and magnetic data that the WVSZ is a northern extension of the Reelfoot Rift (Braile et al., 1982, 1986; Sexton et al., 1986), but others disagree because many of the faults and geophysical anomalies in the WVSZ are truncated by the Rough Creek-Shawneetown fault system to the south (Nelson, 1991; Hillendbrand and Ravat, 1997). The relationship of the WVSZ to deep basement structures and surrounding features such as the Commerce Geophysical Lineament, the Reelfoot Rift, and the Rough Creek Graben remains uncertain.

Paleoseismic History

Paleoseismic studies indicate that the WVSZ experienced at least seven earthquakes with magnitudes >M 6.0 within the past 20,000 years (Fig. 2), with the majority of them occurring during the Holocene (Obermeier et al., 1991, 1993; Munson and Munson, 1996; Munson et al., 1997, Obermeier, 1998; Olson et al., 2005, Counts et al., 2008a). These studies were based on the size and distribution of paleoliquefac

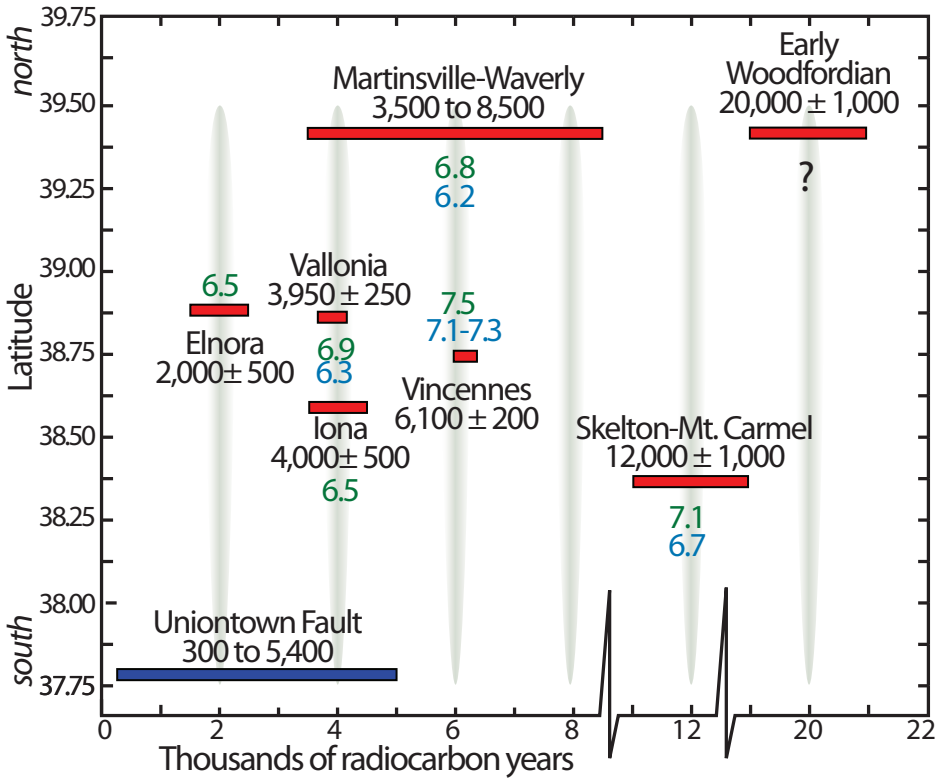

Figure 2. Paleoearthquakes in the WVSZ identified from paleoliquefaction studies (red, Munson and Munson, 1996) and a fault study (blue, Van Arsdale et al., 2008). Green numbers represent back-calculations of earthquake magnitude Olson et al. (2005); blue numbers are magnitude estimates by Munson and Munson (1996).

tion features, which are indicators of very strong shaking (Obermeier, 1996, 2009). However, the study of paleoliquefaction features may be usefult to determine the meisoseismal area of paleoearthquakes, but it does not typically locate seismogenic faults (Obermeier, 2009). Consequently, none of the paleoearthquakes that occurred in the WVSZ can be linked to a specific fault. Recent research has identified Qua-

ternary slip on faults in the WVSZ, but the strength of shaking caused by the slip is unknown. Numerous shallow seismic reflection studies in the WVSZ have identified many faults with up to 10m of offset in bedrock and the overlying alluvium (Woolery et al., 2004; Woolery 2005; Rutledge, 2004; Whitt, 2007). Radiocarbon ages of the offset Quaternary horizons that could be sampled by drilling ranged from 1,100 to 42,000 yrs. BP (Rutledge, 2004; Woolery, 2005).

Modern Seismic Activity

The WVSZ has produced eight M5.0 to 5.5 earthquakes and dozens larger than M 4.0 within the past 175 years (Fig. 3) (Wheeler et al., 1997; Dart and Volpi, 2010). Most of these earthquakes were deeply seated and originated in the Precambrian basement, and only two of all the instrumentally recorded earthquakes have occurred on mapped faults (Bear et al., 1997; Mitchell et al., 1991 Taylor et al., 1989; Kim, 2003; Yang et al., 2009), suggesting that the WVSZ has many unknown seismogenic faults. Some researchers believe that strain from the NMSZ is transferring to the WVSZ, explaining the large number of recent M4.0–5.0 earthquakes in the WVSZ, and speculate that the next large earthquake in the CEUS will be within the WVSZ (Li et al., 2005; 2007).

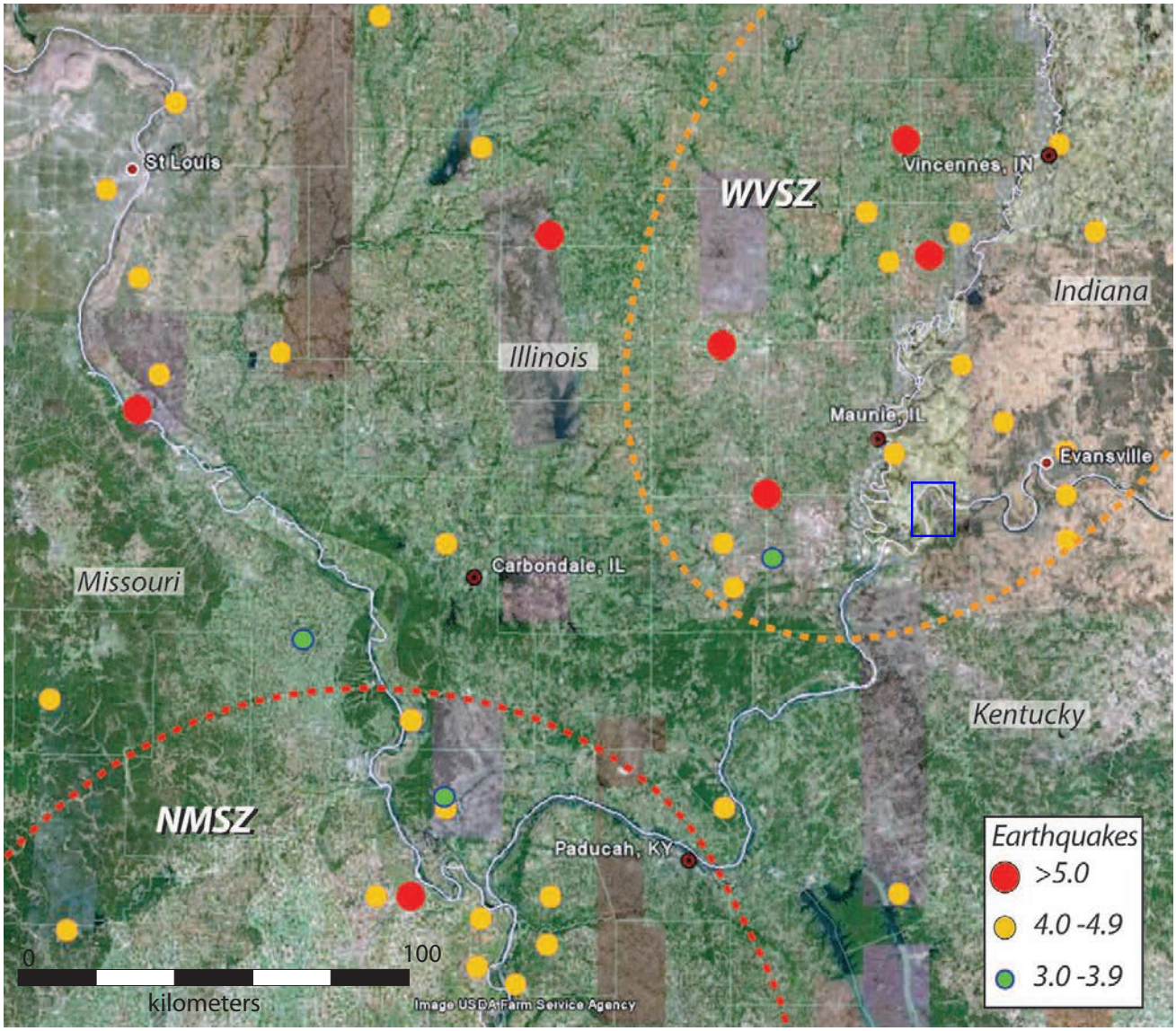

Figure 3. Paleoearthquakes in the WVSZ identified from paleoliquefaction studies (red, Munson and Munson, 1996) and a fault study (blue, Van Arsdale et al., 2008). Colored numbers represent back-calculations of paleoearthquake magnitudes (Olson et al., 2005)

The Uniontown Fault

Background

Geologic mapping near the confluence of the Ohio and Wabash Rivers in 2006 by the PI (Counts) identified an unusual north–south-trending, approximately 2-m-high scarp with down-to-the-west displacement (Fig. 4A). The scarp appeared to be an erosional terrace scarp formed by the Ohio River, but this interpretation is not supported by field relationships and geomorphic evidence. Many well-defined, east-west drainage channels can be traced across the scarp and onto the western, lower side where they were less obvious and muted by annual flooding (Fig. 4B). This suggests that both sides of the scarp were once at the same elevation, because if the scarp was an erosional feature, drainage patterns on the western side of the scarp should have north-south orientations. Geomorphic features suggest the Ohio River flowed south for a relatively long period as it migrated westward across a broad alluvial valley with thick sedimentary fill. Then, a perturbation abruptly shifted the channel nearly 180º on a path that clearly flows around the scarp in three straightened channel sections, and then the channel returns to nearly the same position it occupied before the abrupt diversion (Counts et al., 2008b). This is a common geomorphic response of meandering rivers to surface deformation (Holbrook and Schumm, 1999), and is analogous to how the Mississippi River flows around the Kentucky Bend Scarp of the Reelfoot Fault at New Madrid, Mo. (Kelson et al., 1994). The anomalous scarp itself is almost perfectly straight for 5 km (Fig. 4D), and it lies within the active floodplain where there should be point-bar deposition instead of an erosional terrace. There are no realistic geomorphic solutions or explanations for the existence of this scarp as a fluvial landform given the current configuration of the Ohio River, the surrounding landforms, and surficial deposits in the surrounding area.

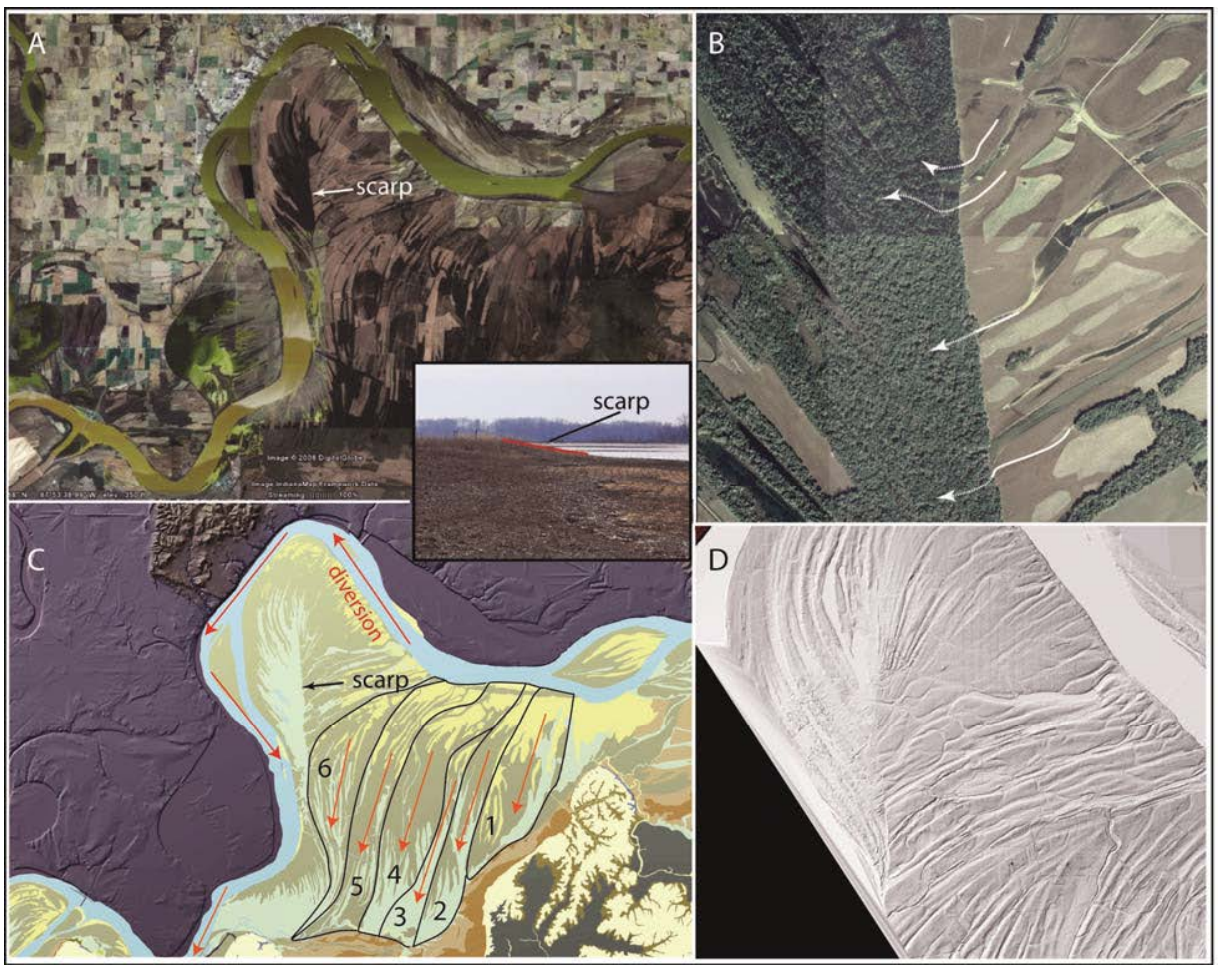

Figure 4. A. The north–south-trending scarp of the Uniontown Fault in the Ohio River floodplain. B. Drainage patterns are continuous across the scarp, suggesting it was formed by faulting and not erosion. C. Geomorphic sequences 1 through 6 show a south-flowing and west-migrating Ohio River. After the deposition of sequence 6, the river abruptly flows north, around the scarp, and returns to its former position. D. High-resolution digital terrain model of the fault scarp created by photogrammetry on 2 ft/pixel aerial imagery.

Dr. Roy Van Arsdale (University of Memphis) had funding to open a trench across the fault scarp, in collaboration with Counts, when his initial trenching target for NEHRP project 07HQGR0052 became inaccessible. Seismic reflection data acquired with static geophones were used to select a suitable site for the trench, and in October 2008 Van Arsdale and Counts opened a 33-m-long, 2.5-m-deep trench across the scarp (Van Arsdale et al., 2009). The trenching exposed a deformed paleosol and alluvium that were folded into a down-to-the-west monocline with approximately 3 m of structural amplitude. Limited funding allowed for only three AMS radiocarbon dates, so one sample from each unit exposed in the trench was selected for ^{14}C dating. Radiocarbon dating indicate that the folding observed in the trench occurred in the late Holocene after 3,745 ±25 yrs BP, with possible minor fault reactivation 295 ±25 yrs BP (Van Arsdale et al., 2008). The fault was named the Uniontown fault, and it is interpreted as splay or step-over fault that connects two mapped faults within the Hovey Lake fault system.

The goal of this project was to use a multi-disciplinary approach involving sedimentology, geophysics, and luminescence dating to extend the paleoseismic record of the Uniontown fault and determine a longer-term slip history.

Methods

Sediment Cores

Eight sites spaced approximately 5 m apart were cored along a transect adjacent (and parallel) to the 2008 trench site (Fig. 5). The cores ranged from 9 – 13.5 m deep. Cores were obtained using a trailer-mounted, Giddings 25-SCT HDGSRPST hydraulic soil sampling, coring, and drilling system. The drill has been customized with a modified Livingston-type piston core-sampling system that enhances core recovery in sediments that can be difficult to core using direct-push methods, and the piston also prevents core contamination from borehole collapse or scraping the sidewall. Clear polycarbonate tubing was used to line the core barrels. After drilling, natural gamma logs were acquired down the boreholes using a Mount Sopris portable gamma-logging system.

Magnetic Susceptibility

The cores were taken to Vanderbilt University and processed on a GEOTEK MSCL (Multi-Sensor Core Logger) system equipped with a Bartington MS2C loop magnetic susceptibility (MS). MS measurements were done on whole cores at a 2 cm interval. The cores were then split and described in the KGS sediment characterization lab in Henderson, KY.

Electrical Resistivity

Electrical resistance (ER) is a good proxy for grain size and can work extremely well for mapping glaciofluvial environments (Baines et al., 2003). ER is also effective at identifying offset in bedrock surfaces and thick Quaternary sedimentary units (Suzuki et al., 2000). ER profiles ~325 m long were measured adjacent to the 2008 trench site using an AGI Supersting R8 IP 8 channel earth resistivity and IP meter. The ER system has 84 electrodes which were spaced 4 meters apart. The first profile was measured using a Wenner array. The electrodes were left in place, and a second profile was measured using a Schlumberger array. Inversions were done using EarthImager 2D software.

Ground Penetrating Radar (GPR)

A 25 meter long GPR profile was acquired across the scarp using a Sensors and Software pulseEKKO PRO system uses 200, 100, and 50 MHz antennae. The profile was positioned so the center of the GPR profile was at the center of the scarp, and the factory recommended spacing of the antennae was used for each array.

Seismic Reflection

More than 2 km of S-wave seismic reflection data were acquired along two profiles perpendicular to the fault, one north and one south of the 2008 trench site (Fig. 5). Seismic data were acquired using the Illinois State Geological Survey's S-wave land streamer system. The system consists of 24 horizontally polarized geophone pairs mounted on 3-lb steel sleds spaced at 3-foot intervals. The source is a horizontally-struck hydraulic ram-loaded roller spaced 5 feet from the first geophone (Pugin et al., 2002). The source and streamer are towed together behind the acquisition vehicle, and the ram-loaded roller is struck in 5-foot intervals, resulting in a 6 CMP fold of coverage and CMP bin size of 1.25 feet.

Figure 5. Natural color satellite image of the study area showing the Uniontown Fault and locations of seismic reflection profiles, a GPR profile, electrical resistivity profiles, and OSL sample sites. Image courtesy of the Advanced Land Imager on NASA's EO-1 satellite.

Optically Stimulated Luminescence Dating

Optically Stimulated Luminescence (OSL) dating determines the time elapsed since sediments were last exposed to sunlight (Aitken, 1998). The method assumes that mineral grains were exposed to daylight during or immediately prior to transport and relies on the interaction of ionizing radiation with electrons in semi-conducting minerals within buried sediments. This results in the metastable accumulation of electrons within the crystal lattice structure of the minerals that are shielded from daylight. After burial, a luminescence signal begins to accumulate in the crystal lattices due to a background dose of radiation arising from the decay of ambient radioisotopes such as ^{238}U, ^{232}Th, and ^{40}K. Assuming that the radiation exposure (the dose rate - DR) is constant over the timescales of interest, the luminescence signal buildup (equivalent dose – DE) in the minerals is proportional to the duration of burial and the concentration of the radioisotopes in the sample environment. The depositional age (A) of the sample is thus a ratio of equivalent dose acquired and the background dose rate (i.e., A=DE/DR) (Murray & Olley, 2002; Singhvi & Porat, 2008).

Samples for OSL dating must remain shielded from light until they are analyzed in a dark laboratory. To ensure that bioturbation or pedogenesis did not expose sediments to sunlight after burial, OSL samples were taken at depths immediately below the modern soil profile, which was usually between 2 –3 m deep. Sites were cored with a standard Giddings core barrel in 1.25 meter intervals, and the cores were opened and described until unweathered sand was encountered. Then, the standard core barrel was replaced with a 35 cm core barrel assembly equipped with a core catcher. A 30 cm long stainless steel tube was sealed at the top with opaque foil tape and used as a core barrel liner. After the core barrel assembly was driven through the sample interval, it was removed from the drill string, placed under a large black cloth, the liner was removed from the core barrel, and the bottom was sealed with foil tape. Then the sealed tube was labeled and placed in an opaque film bag for transport to the lab.

The OSL samples were taken to the Luminescence Dating laboratory at the University of Cincinnati. Five to ten cm of sediment was removed from each end of the tube and dried to determine the water content of each sample. The sediment was then crushed and sent to the U.S. Geological Survey Denver, Colorado for instrumental neutron activation analysis (INAA) to determine the U, Th and K concentration for DR determination (Table 1). The sediment from the center of the tubes was used for the age analyses and pretreated with 10% HCl and 10% H_2O_2 to remove carbonates and organic material, respectively. The pretreated samples were rinsed in water, dried, and sieved through 90-250 μm screens. This grain fraction was then etched using 44% HF acid for 80 minutes to remove everything but quartz, feldspar, and heavy mineral grains as well as the outer alpha irradiated layer from the quartz grains. Then the samples were treated with concentrated HCl to remove any fluoride precipitates and rinsed with deionized water distilled water and acetate, and dried and sieved to obtain the 90-150μm fraction. Feldspar and magnetic mineral grains were removed from the sample, using a low-field controlled Frantz isodynamic magnetic separator (LFC Model-2), as the sample was passed through a variable magnetic field with forward and side slopes both set at 10° (Porat, 2006). After the magnetic separation was performed three times (to ensure the sample only contained quartz), samples were ready for luminescence measurements.

An automated Risoe TL-DA-20 OSL reader was used for OSL measurements and irradiation. Aliquots, containing approximately several hundred grains of the samples, were mounted onto ~6mm-stainless steel discs as a small central circle approximately 3mm in diameter. Aliquots for each sample were first checked for feldspar contamination using room-temperature IRSL before the main OSL measurements were undertaken (Jain & Singhvi, 2001). Aliquots that did not pass the IRSL test were etched again in 40% HF for an additional 30 minutes to remove feldspar, followed by 10% HCl treatment and sieving

Table1. Equivalent dose and dates estimated using single aliquot regenerative (SAR) method. Each date was estimated feeding data in software by Grün (1991)

Sample	*No_Dsk	Alt (m)	Depth(cm)	Lat.(N)/Lat.(E)	Wt_mean(Gy)	Mean(Gy)	Dose Rate(Gy/ka)	Wt mean(Ka)	Mean(ka)
STL400	21(24)	102.00	400.00	37.85943/-879423	7.1±0.03	7.4±1	1.52 ± 0.01	4.67 ± 0.16	4.86 ± 0.68
LORV-01	24(24)	113.39	259.08	37.8177/-87.7879	20.44 ± 0.05	19.11 ± 3.14	1.28 ± 0.07	15.94 ± 0.87	14.90 ± 2.58
LORV-03	24(24)	109.73	137.16	37.8389-87.8065	12.03 ± 0.02	14.62 ± 3.24	1.25 ± 0.08	9.61 ± 0.58	11.68 ± 2.68
LORV-05	23(24)	109.73	228.60	37.8461/-87.8236	11.05 ± 0.06	11.72 ±1.72	1.35 ± 0.08	8.22 ± 0.50	8.72 ± 1.38
LORV-06	22(24)	109.12	381.00	37.8472/-87.8275	12.68 ± 0.05	13.35 ± 1.62	1.35 ± 0.08	9.38 ± 0.54	9.87 ± 1.32
LORV-07	24(24)	109.42	228.60	37.8525/-87.8385	9.15 ± 0.03	9.95 ± 1.70	0.87 ± 0.05	11.48 ± 0.56	11.93 ± 2.14
LORV-08	24(24)	107.29	228.60	37.8266/-87.8447	16.32 ± 0.03	17.03 ± 2.98	1.66 ± 0.10	9.84 ± 0.61	10.27 ± 1.91
LORV-09	24(24)	108.81	472.44	37.8199/-87.8516	9.77 ± 0.03	10.08 ± 1.01	1.39 ± 0.16	7.02 ± 0.80	7.25 ± 1.09
LORV-10	24(24)	110.34	228.60	37.8420/-87.8577	10.56 ± 0.03	11.72 ± 1.93	1.71 ± 0.09	6.18 ± 0.34	6.59 ± 1.15
LORV-11	23(24)	110.03	228.60	37.8366/-87.8726	19.90 ± 0.08	20.04 ± 2.74	1.33 ± 0.07	14.93 ± 0.83	15.03 ± 2.22
LORV-12	24(24)	109.73	198.12	37.8458/-87.7350	14.05 ± 0.03	14.72 ± 1.74	1.58 ± 0.10	8.91 ± 0.58	9.34 ± 1.26
LORV-13	21(24)	109.42	411.48	37.8571/-87.8420	7.00 ± 0.02	7.12 ± 0.51	1.74 ± 0.11	4.01 ± 0.24	4.08 ± 0.38
LORV-14	23(24)	109.12	320.04	37.8727/-87.8683	7.51 ± 0.02	7.77 ± 0.97	1.30 ± 0.08	5.76 ± 0.37	5.96 ± 0.84
LORV-15	21(24)	109.73	289.56	37.8702/-87.8683	6.45 ± 0.03	6.67 ± 0.71	1.51 ± 0.09	4.27 ± 0.22	4.42 ± 0.52
LORV-16	20(24)	109.73	167.64	37.8753/-87.8693	21.67 ± 0.12	21.78 ± 3.10	1.61 ± 0.08	13.45 ± 0.79	13.52 ± 2.08
LORV-17	24(24)	110.64	381.00	37.7984/-87.8192	36.52 ± 0.17	36.83 ± 4.55	2.19 ± 0.13	16.70 ± 0.98	16.84 ± 2.30
LORV-18	23(24)	114.60	381.00	37.7792/-87.8192	15.63 ± 0.05	16.4 ± 2.30	1.16 ± 0.06	13.52 ± 0.74	14.19 ± 2.13
LORV-19	24(24)	109.73	198.12	37.8471/-87.7970	9.62 ± 0.03	12.94 ± 3.03	1.21 ± 0.07	7.96 ± 0.46	10.71 ± 2.58
LORV-20	23(24)	110.03	426.72	37.8472/-87.8806	7.64 ± 0.04	8.08 ±1.32	1.02 ± 0.06	7.47 ± 0.41	7.90 ± 1.36
LORV-21A	24(24)	109.73	259.08	37.8461/-87.8903	9.12 ± 0.02	9.8 ± 1.24	0.83 ± 0.04	10.97 ± 0.58	11.79 ± 1.62
LORV-21B	20(24)	109.73	259.08	37.8461/-87.8903	7.99 ± 0.02	8.24 ± 0.84	0.65 ± 0.04	12.30 ± 0.72	12.68 ± 1.49
LORV-22	22(24)	106.68	198.12	37.8675/-87.9108	1.69 ± 0.01	1.72 ± 0.17	0.87 ± 0.05	1.94 ± 0.11	1.97 ± 0.22
LORV-23	24(24)	107.59	502.92	37.8966/-87.9176	1.84 ± 0.01	1.88 ± 0.18	1.12 ± 0.06	1.65 ± 0.09	1.69 ± 0.19
LORV-24	19(24)	108.20	228.60	37.8933/-87.8842	3.91 ± 0.04	4.21 ± 0.71	0.54 ± 0.03	7.27 ± 0.47	7.83 ± 1.41
LORV-25	23(24)	107.90	502.92	37.8829/-87.8842	8.16 ± 0.03	8.14 ± 0.98	1.30 ± 0.07	6.28 ± 0.33	6.26 ± 0.82

again. Samples that passed IRSL test were used for OSL dating. Aliquots of samples were illuminated with blue LEDs (blue light stimulated luminescence – BLSL) and irradiated using a $^{90}Sr/^{90}Y$beta source. The single aliquot regeneration (SAR) method of Murray and Wintle, (2000) was used to determine the equivalent dose for age estimation. Only aliquots with a recycling ratio less than 10% were used in determining DE. A preheat of 240 ^{o}C for 10s was used and the OSL signal was recorded for 40s at 125°C. OSL sensitivity of the samples had a high signal to noise ratio. Dose recovery tests (Wintle & Murray, 2006) indicate that a laboratory dose could be recovered to within 2% by the SAR protocol suggesting that the protocol was appropriate. The OSL ages used in this report are the mean age from all the aliquots recorded for each sample, and the uncertainty is the standard error.

Results

Sediment Cores

Coarse saturated sands made drilling conditions difficult, and the original target of obtaining 15 m cores could not be accomplished. Drill refusal usually occurred on pebble sand at around 9 meters deep. Drilling in loose, non-cohesive sediments required the use of a core-catcher, and this resulted in an unforeseen situation regarding changes in core diameter during drilling. The diameter of the cutting bit assembly for the core-catcher is 3 cm, which is 1 cm smaller than the 4 cm diameter of the core liners. Consequently, the non-cohesive sediments expanded into the core barrel, but the cohesive sediments did not, and this resulted in compression, or shortening, of some sections of the core by as much as 46 cm per meter of core. Therefore, when the length of the core was less than the drive interval, sometimes it was difficult to determine if part of the core was lost or if the core compressed. Corrections were made for the compression, but errors within each drive interval could be off by as much as a half meter, resulting in a degree of uncertainty about stratigraphic correlations between cores.

Core descriptions (appendix A) consistently identified four stratigraphic units in the cores east of the scarp: silt, loamy sand, clay, and coarse basal sand. A clay bed with fine sand laminae was a diagnostic marker bed that appears to be at a constant elevation in the six easternmost cores (Fig 6). In core 12-003 in the middle of the scarp, the top of this clay bed is ~1.0 meters lower, a trend that mimics the surface topography.

The stratigraphy in cores 12-003 and 12-004 on the western side of the scarp was more complex. Fine-grained units were thicker, more variable, and the sand was typically finer and had better sorting. The paleosol exposed in the 2008 trench was identified in both of these cores, and the paleosol was down-to-the-west as was observed in the 2008 trench (Fig 6).

Magnetic Susceptibility and Natural Gamma

Magnetic susceptibility can be an excellent tool for correlation between cores. The MS of the core plugs cannot be logged using the same technique as the whole cores, so the MS of the plugs was not measured. Compressed cores cannot be decompressed for MS logging, but corrections were made for compression in the core descriptions and graphic logs, so the MS curves may not precisely match the graphic logs, creating further uncertainty in correlations. Despite these complications, there are a set of MS peaks in the upper and lower sand intervals that can be traced across the cores (Fig. 6). Like the paleosol, these peaks appear to be folded in a down-to-the-west monocline.

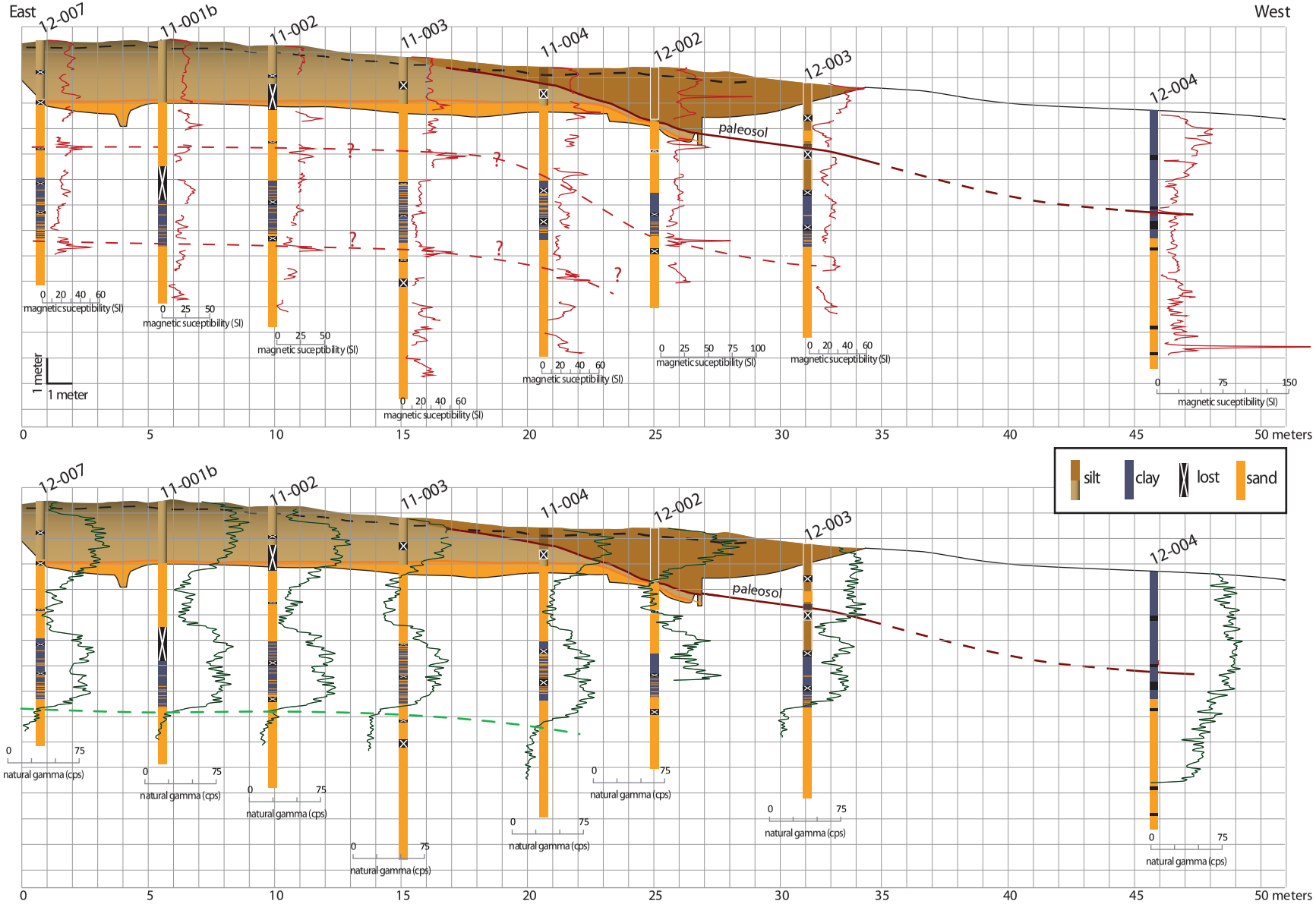

Figure 6. Simplified stratigraphic logs of sediment cores, magnetic susceptibility measurements (red) and natural gamma

Natural gamma curves are a proxy for grain size and are useful for correlations in glaciofluvial environments (Bleuer, 2004), especially when there are intervals of missing core. The gamma curves for the first 5 boreholes, from east to west, are all very similar and consistent with observations from the sediment cores (Fig 6.). The top of the basal sand in the 5th core (11-004) appears to be ~30 cm lower, which is the same trend seen in the MS curves but not as pronounced. The natural gamma curves for the remaining cores are not as deep, so this trend could not be traced farther west through the remaining cores.

Ground penetrating radar

Although antennae arrays of 200, 100, and 50 MHz antennas were used to collect GPR data, water from a recent rain impeded the signal from the 100 and 200 MHz arrays, and only the 50 MHz antennae produced a GPR profile with clear data. There are three distinctive characteristics in the reflectors of this profile. Reflectors on the eastern side of the scarp are clear and distinct to a depth nearly twice as deep as reflectors on the western side of the scarp (Fig. 7). Reflectors at ~9 m are kinked, and reflectors at ~18 m are offset. Reflectors between 9 m and 18 m appear warped or distorted, and this area lies beneath the scarp at the surface.

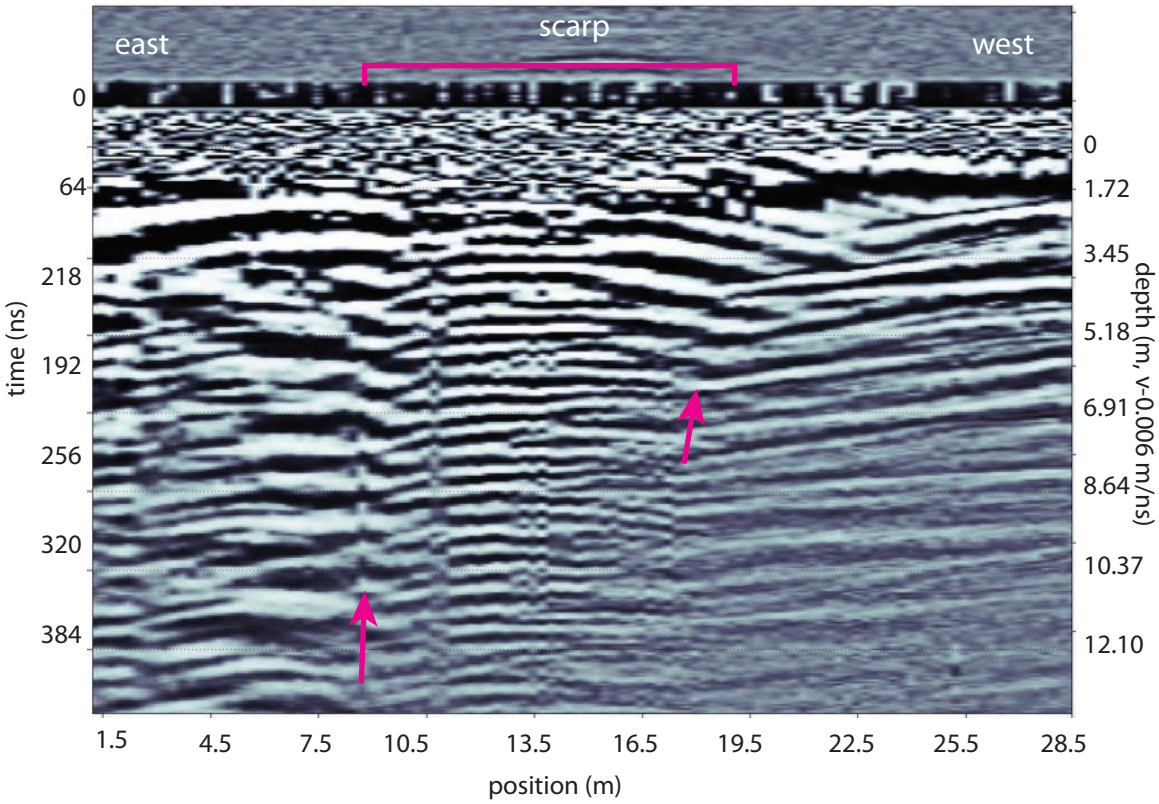

Figure 7. GPR profile parallel to the trench site acquired with 50 MHz antenna array. Reflectors beneatht he scarp differ from reflectors to the east and west, and the area under the scarp has the morphology of a graben or half-graben.

Electrical Resistivity

The inverted ER profiles for the Wenner and Schlumberger arrays are similar to one another near the surface, but the Schlumberger profile is more detailed at depth and shows patterns that can be related to the bedrock surface and possibly sand and clay above bedrock (Fig. 8). The Schlumberger profile shows a very large downward step in the bedrock surface beneath the scarp. A much smaller downward step is also apparent in the near-surface sand bed beneath the scarp.

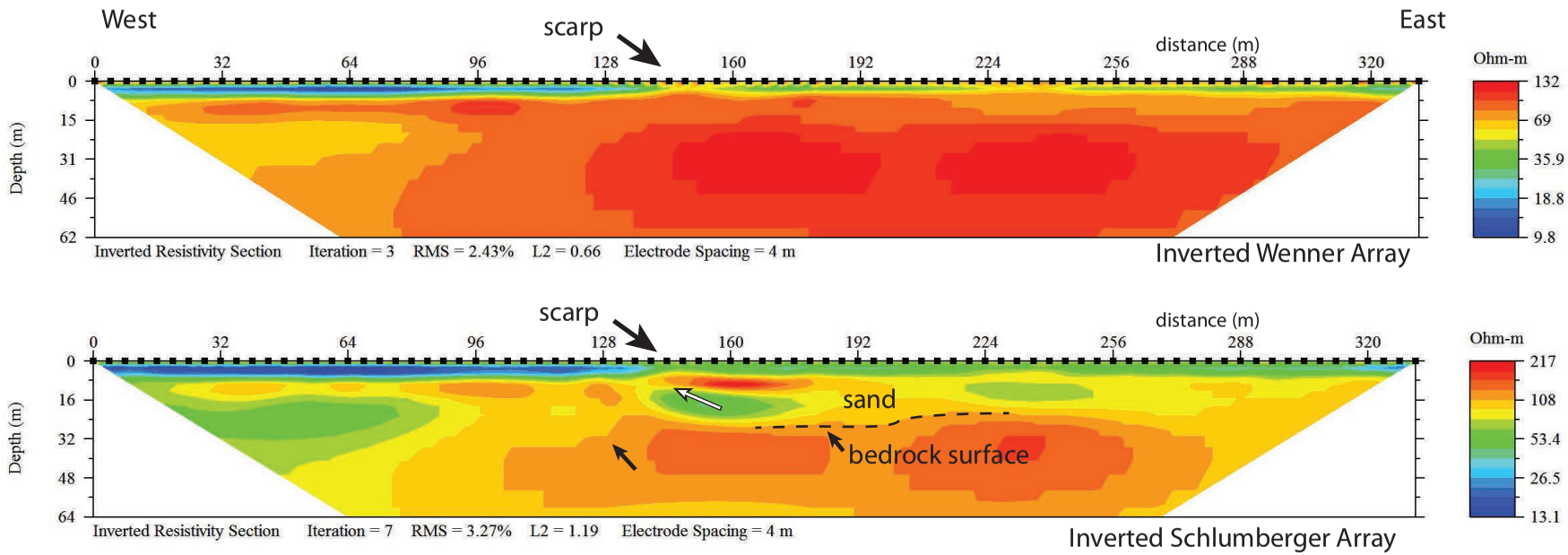

Figure 8. Inverted ER profiles show downward steps in the bedrock surface and at the top of the sand beneath the scarp.

Seismic Reflection

The ISGS S-wave land streamer system requires paved or gravel roads, so a seismic profile could not be collected across the scarp. Seismic data were collected perpendicular to the fault on gravel roads to the north and south of the 2008 trench site (Fig. 5). The northern seismic profile displays offset in the bedrock surface in several locations. The offset ranges from 3-4 meters and has horst-and-graben characteristics (Fig. 9). The surface expression of the fault becomes muted and eventually disappears northward, but there is offset at the western end of this seismic profile that corresponds to where the Uniontown Fault would cross the profile if it was projected north.

The southern seismic profile is 200 m longer than the northern profile and includes a slight change in direction that resulted in a 25 m section of lost data. Despite this gap, the data are excellent and show offset in the bedrock surface in multiple locations, including a fault complex just to the east of the scarp (Fig. 10). Reflectors under the scarp appear extremely distorted, and there appears to be a fault at the base of the scarp, but this could also be an artifact from the small culvert where the road crosses a drainage ditch. Seismic profiles collected by the ISGS land streamer in western Kentucky in previous years produced very high-resolution reflection profiles that showed subsurface details such as cross bedding, point bars, sediments on lapping an irregular bedrock surface. Windy conditions during seismic acquisition resulted in significant background noise, preventing the acquisition of such details in these seismic lines.

Geochronology

Sediments recovered along the coring transect appeared to have been deformed by the same event that deformed the land surface. Data from nearby oil and gas wells indicate sediments at the trench site are nearly 40 m thick, so our coring only penetrated ~35% of the total sediment package. Because our cores were not deep enough to recover sediments deformed by older events, a different approach was employed to seek evidence for older earthquake events on the Uniontown fault.

Alluvial rivers (such as the Ohio River) that flow unrestricted on thick alluvium are largely unaffected by bedrock controls and tend to quickly establish equilibrium conditions between erosional and resistant forces (Schumm, 1985). This makes alluvial rivers particularly sensitive to faulting and neotectonic deformation, because even the most subtle changes in the land surface can alter the gradient, and the rivers respond to the new conditions in predictable ways (Schumm et al., 2000). These responses include changes in the longitudinal profiles, abrupt changes in channel morphology, flow diversions, shifting position in the valley, and changes in sedimentation styles or sedimentation rates (Holbrook and Schumm, 1999; Schumm et al., 2000).

Twenty-five samples for OSL dating were collected from point bar ridges surrounding the Uniontown Fault to develop a chronology of depositional changes and to see if they could be linked to slip on the Uniontown fault. An OSL sample that was collected from the sand unit exposed in the bottom of the 2008 trench was also analyzed (STL400).

OSL ages were obtained for all but two of the samples analyzed: samples LORV 02 and LORV 04 did not contain enough 90-150μm sand to measure a luminescence signal. For all other samples, the grains were bright (had high signal to noise ratios) and had been sufficiently exposed to sunlight to reset the luminescence signal prior to burial.

OSL ages of deposits surrounding the scarp ranged from 15.8 ka to 1.5 ka (Table 2). To test for stratigraphic consistency, two samples vertically separated by 20 cm were measured from LORV 21 (A and B)

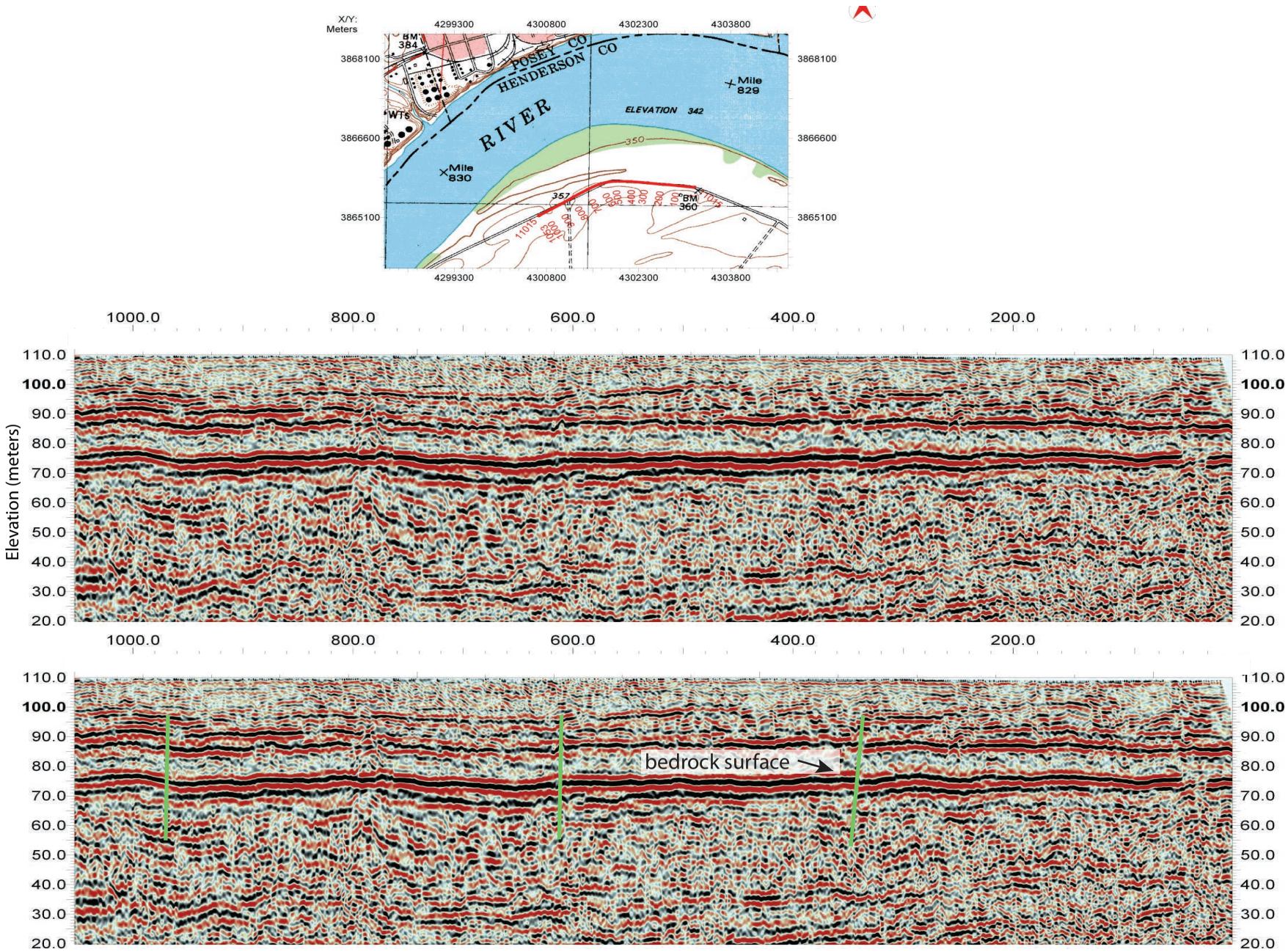

Figure 9. S-wave seismic reflection profile across the northern end of the scarp next tohte Ohio River. The bedrock surface and some overlying Quaternary reflectors have minor offset. Green lines represent faults.

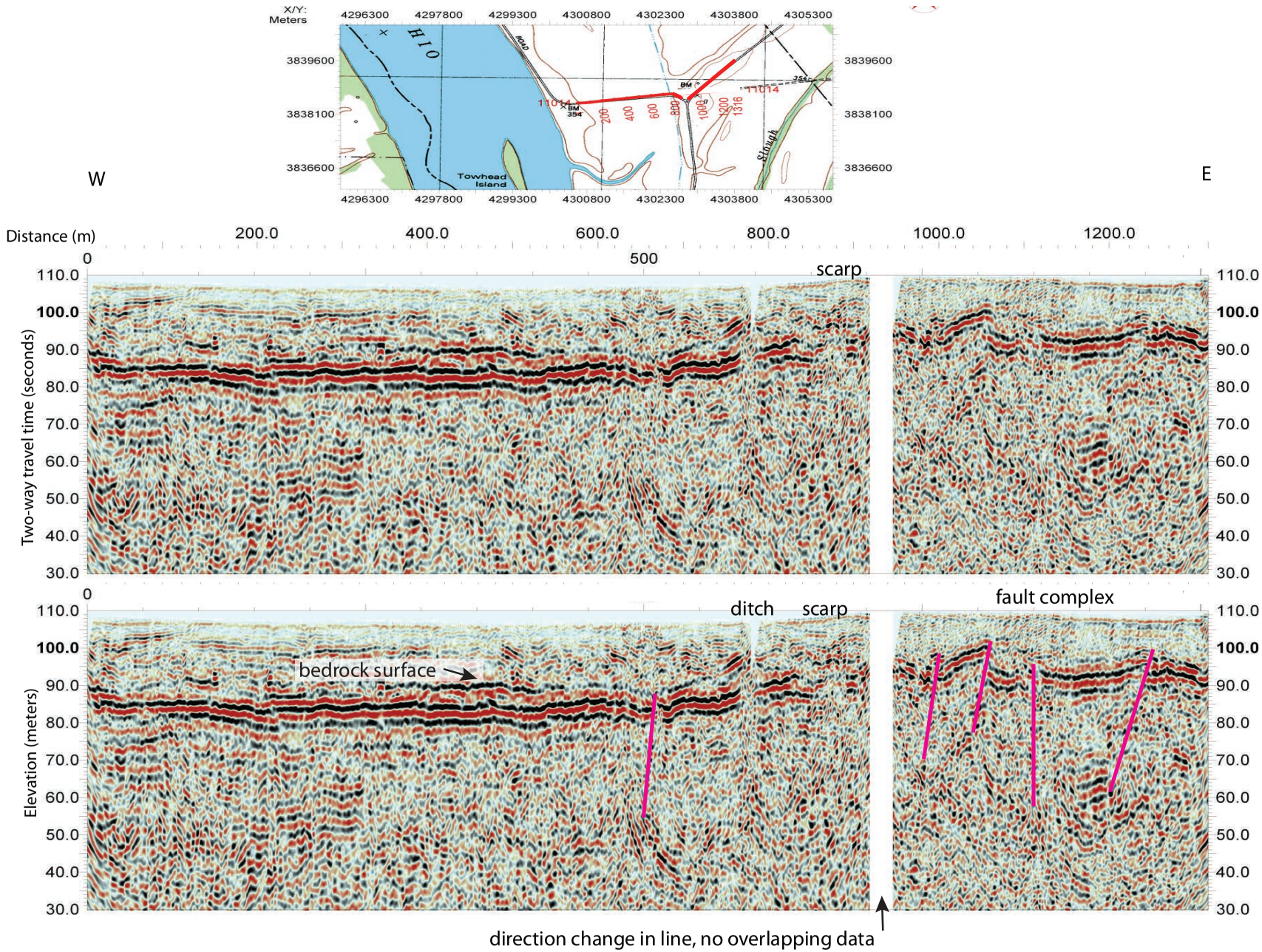

Figure 10. S-wave seismic reflection profile across the southern end of the scarp. Bedrock and overlying reflectors appear to be offset beneath the scarp. A fault complex with significant offset lies approximately 200 m east of the scarp. Pink lines represent faults.

Table 2. Radioisotope, water content, cosmic dose data, and the calculated dose-rate for samples. Water content used is at the time of sample collection and dose rate is estimated using Prescott and Hutton (1994). Complete dose rate was estimated using software written by Grun (1991).

Sample	U(ppm)			Th(ppm)			K%			Water Content(%)			Cosmic(μGy/a)			Dose Rate(Gy/ka)		
STL400	1.70	±	0.017	4.80	±	0.05	0.90	±	0.01	10.00	±	2.00	104	±	21	1.52	±	0.01
LORV-01	1.12	±	0.11	2.95	±	0.30	0.78	±	0.04	4.78	±	0.96	133	±	27	1.28	±	0.07
LORV-03	1.29	±	0.13	3.38	±	0.34	0.71	±	0.04	8.94	±	1.79	163	±	33	1.25	±	0.08
LORV-05	1.42	±	0.14	4.05	±	0.41	0.79	±	0.04	10.25	±	2.05	139	±	28	1.35	±	0.08
LORV-06	1.36	±	0.14	3.98	±	0.40	0.76	±	0.04	5.14	±	1.03	109	±	22	1.35	±	0.08
LORV-07	0.62	±	0.06	1.75	±	0.18	0.49	±	0.02	1.45	±	0.29	139	±	28	0.87	±	0.05
LORV-08	1.92	±	0.19	5.76	±	0.58	0.90	±	0.05	9.44	±	1.89	139	±	28	1.66	±	0.10
LORV-09	1.71	±	0.17	4.91	±	0.49	0.81	±	0.04	12.34	±	2.47	95	±	19	1.39	±	0.16
LORV-10	1.70	±	0.17	5.29	±	0.53	0.89	±	0.04	2.47	±	0.49	139	±	28	1.71	±	0.09
LORV-11	1.23	±	0.12	3.31	±	0.33	0.74	±	0.04	2.43	±	0.49	139	±	28	1.33	±	0.07
LORV-12	1.85	±	0.19	5.52	±	0.55	0.90	±	0.05	12.59	±	2.52	147	±	29	1.58	±	0.10
LORV-13	2.07	±	0.21	5.82	±	0.58	0.98	±	0.05	8.59	±	1.72	104	±	21	1.74	±	0.11
LORV-14	1.45	±	0.15	4.16	±	0.42	0.80	±	0.04	12.94	±	2.59	120	±	24	1.30	±	0.08
LORV-15	1.31	±	0.13	3.5	±	0.35	0.88	±	0.04	0.79	±	0.16	126	±	25	1.51	±	0.09
LORV-16	1.78	±	0.18	4.15	±	0.42	0.92	±	0.05	6.91	±	1.38	155	±	31	1.61	±	0.08
LORV-17	2.47	±	0.25	6.02	±	0.60	1.38	±	0.07	8.85	±	1.77	109	±	22	2.19	±	0.13
LORV-18	0.93	±	0.09	2.55	±	0.26	0.70	±	0.04	1.81	±	0.36	109	±	22	1.16	±	0.06
LORV-19	0.98	±	0.10	2.83	±	0.28	0.80	±	0.04	9.66	±	1.93	147	±	29	1.21	±	0.07
LORV-20	0.75	±	0.07	2.38	±	0.24	0.57	±	0.03	1.34	±	0.27	147	±	29	1.02	±	0.06
LORV-21A	2.06	±	0.21	5.85	±	0.59	0.91	±	0.05	3.46	±	0.69	102	±	20	0.83	±	0.04
LORV-21B	1.55	±	0.16	3.94	±	0.39	0.65	±	0.03	1.61	±	0.32	132	±	26	0.65	±	0.04
LORV-22	2.06	±	0.21	6.01	±	0.60	0.90	±	0.05	4.71	±	0.94	147	±	29	0.87	±	0.05
LORV-23	2.84	±	0.28	8.97	±	0.90	1.31	±	0.07	6.65	±	1.33	91	±	18	1.12	±	0.06
LORV-24	1.00	±	0.10	2.21	±	0.22	0.72	±	0.04	0.98	±	0.20	139	±	28	0.54	±	0.03
LORV-25	3.33	±	0.33	10.6	±	1.06	1.52	±	0.08	6.10	±	1.22	91	±	18	1.30	±	0.07

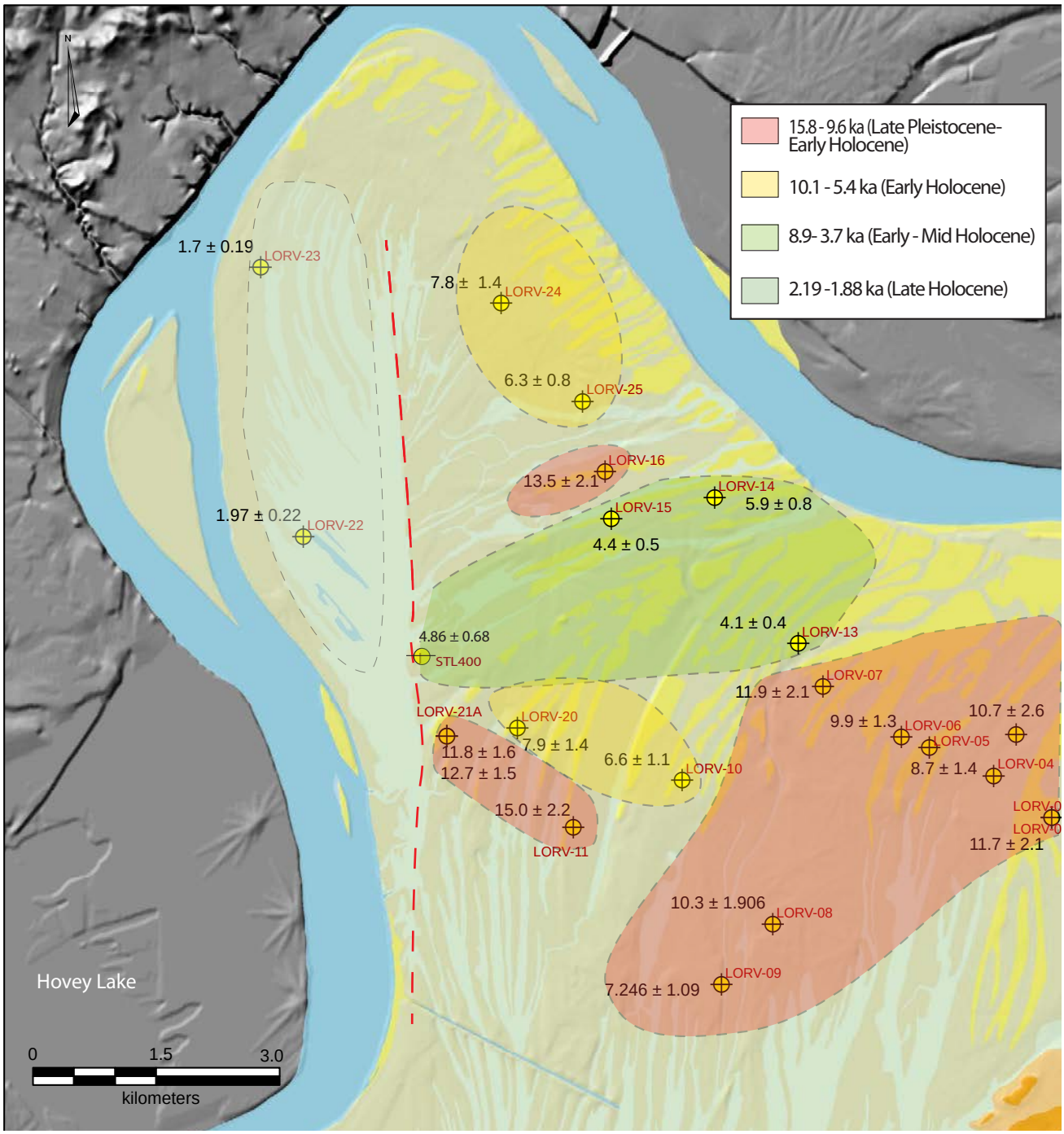

Figure 11. OSL chronology of deposits and landforms surrounding the Uniontown Fault.

and the deeper sample produced an older age. Ages are also laterally consistent and generally fit with surrounding geomorphic patterns, and the calibrated radiocarbon ages from the 2008 trench (4,088 ±57) overlap with the OSL age from the trench (4.86 ±0.68).

Discussion

Data from core descriptions, magnetic susceptibility, and gamma logs show that sediments beneath the trench site mimic the folding that was observed in the 2008 trench. Coring could only penetrate depths ranging from 9 – 13 m, which is roughly the top third of the total sediment thickness beneath the study area. No sedimentary layers were identified as deformed by earlier fault movements in the sediment cores. If sediments were deformed by older slip events on the Uniontown Fault, they are at depths greater than 10 m.

GPR reflection signatures of sediments beneath the scarp are distinctly different than reflection signatures east and west of the scarp (Fig. 7). Sandy sediments east of the scarp have distinct reflectors to a depth of 10 m. West of the scarp sediments contain more silt and clay, and reflectors become obscure below 5 m. Reflectors beneath the scarp are offset such that the region beneatht he scarp looks like a graben or half graben that is ~10 m wide, and the offset is as shallow as 5 m. This offset was not apparent in the sediment cores, however. It is not clear whether the core spacing of 5 m missed the offset reflectors, if the offset was not recognized in the cores due to compression, or if the offset reflectors are an artifact caused by errors during data acquisition or processing.

The Schlumberger ER profile was more detailed than the Wenner ER profile. Sand, clay, and the bedrock surface are clearly visible in the Schlumberger profile. Both the bedrock surface and the top of the upper sand unit step downward beneath the scarp at the surface, but the step at the bedrock surface is nearly three times as large (Fig. 8). It is plausible that this difference represents multiple slip events at the bedrock surface and one slip event on the top of the sand. It is also possible that the offset in the sand and the bedrock were created by the same slip event, with the sand above bedrock accommodating some of the slip, resulting in less offset near the surface.

Both s-wave seismic reflection profiles show offset in the bedrock surface and in reflectors above bedrock, but the offset is much more pronounced in the southern profile (Figs. 9-1). This trend is also reflected at the surface: the height of the scarp is ~2 m at its southern end, and the height progressively decreases northward until it eventually disappears. Initially it was presumed that the northern end of the scarp was buried by sediment because it was closer to the Ohio River, thereby receiving more overbank floodplain sediment. However, the seismic reflection data suggests slip was larger on the southern end of the fault, suggesting the Uniontown fault is part of an accomodation zone. This is consistent with our initial interpretation that the Uniontown fault is a stepover fault connecting two faults in the Hovey Lake Fault System.

The southern seismic profile also reveals multiple faults within a narrow zone 200 m east of the fault scarp. Quaternary reflectors above the fault complex are discontinuous and also appear to be offset, but there is no evidence of deformation at the surface.

OSL ages around the scarp cluster into four distinctive time intervals: late Pleistocene to early Holocene (15.8 –8.2 ka), early Holocene (10.1 – 5.4 ka), early to mid-Holocene (8.9 – 3.7 ka), and late Holocene (2.19 – 1.88 ka) (Table 2). The standard errors range from 200 to 2000 years and many of the ages overlap, but four fluvial landforms of different ages can be roughly outlined using the OSL chronology (Fig 11). The outlined landforms only generally coincide with the surface morphology because the region is still in the active floodplain, but trends are detectable. The late Pleistocene, early Holocene, and mid-

Holocene units were only identified on the eastern side of the scarp. The mid Holocene unit was folded in the 2008 trench, so the other older units were likely folded as well. The late Holocene unit is lower in elevation than the older units and is only found on the western side of the fault, which indicates it was deposited after faulting, so faulting occurred between the deposition of the early and late Holocene units (5.5 – 1.5 ka).

Conclusions and Future Work

The Uniontown fault is an active fault in the Ohio River floodplain. The surface expression of the scarp and seismic reflection data indicate offset along the fault increases southward, suggesting the Uniontown fault is part of a transfer zone that connects the larger mapped faults that lie to the north and south. Sediments potentially offset by older earthquakes are deeper than 13 m below the surface.

The Uniontown fault has affected the geomorphology of the Ohio River. OSL dating indicates the modern channel course of the Ohio River around the Uniontown fault was established between 5.5 and 1.5 ka, the same time inteval of recent slip on the Uniontown fault. OSL dating also shows there has been four phases of fluvial landform development since the late Pleistocene, and these could represent fluvial adjustments to older paleoearthquakes. Additional OSL dating would help to resolve the timing of these changes.

Seismic reflection profiles are currently being reprocessed with new algorithms to try to remove noise and enhance reflectors in the profiles to see if additional trenching targets can be located. Also, the fault complex revealed in the southern seismic reflection profile showed significant offset in the bedrock surface and overlying reflectors and is an excellent trenching target that should be investigated.

The OSL chronology should be expanded in the field area, including on the western side of the scarp in southern Indiana, to seek older fluvial landforms and see if they can be linked to earthquake events. Likewise, the analysis of sediment cores from Hovey Lake, (located just southwest of the Uniontown fault), could identify anomalous sedimentation changes caused by faulting.

References Cited

Aitken, M.J., 1998, An introduction to optical dating: The dating of Quaternary sediments by the use of photon-stimulated luminescence: Oxford, Oxford University Press, 267 p.

Baines, D., Smith, D., Froees, D., Bauman, P., and Nimeck, 2002 Electrical resistivity ground imaging (ERGI): A new tool for mapping the lithology and geometry of channel-belts and valley-fills: Sedimentology, v. 49, no. 3, p. 441–449.

Bear, G., Rupp, J., and Rudman, A., 1997, Seismic interpretation of the deep structure of the Wabash Valley fault system: Seismological Research Letters, v. 68, p. 624-640.

Braile, L., Keller, G., Hinze, W., and Lidiak, E., 1982, An ancient rift complex and its relation to contemporary seismicity in the New Madrid seismic zone: Tectonics, v. 1, p. 225-237.

Braile, L.W., Hinze, W.J., Keller, G.R., Lidiak, E.G., and Sexton, J.L., 1986, Tectonic development of the New Madrid rift complex, Mississippi embayment, North America: Tectonophysics, v. 131, p. 1-21.

Bristol, H.M., and Treworgy, J.D., 1979, The Wabash Valley Fault System in southeastern Illinois: Ur-

bana, Ill., Illinois Institute of Natural Resources, Illinois State Geological Survey Division.

Bleuer, N., 2004, Slow logging of subtle sequences: The gamma-ray log character of glacigenic and other unconsolidated sedimentary sequences: Indiana Geological Survey Special Report 65, 39 p.

Counts, R.C., Durbin, J.M., and Obermeier, S.F., 2008a, Seismic ground-failure features in the vicinity of the lower Wabash and Ohio River Valleys, in Maria, A.H., and Counts, R.C., eds., From the Cincinnati Arch to the Illinois Basin: Geological field excursions along the Ohio River Valley: Geological Society of America Field Guide 12, p. 57–79.

Counts, R.C., Woolery, E., and Van Arsdale, R., 2008b, Quaternary faulting in Union County, KY: Preliminary results [abs.]: Geological Society of America, Abstracts with Programs, v. 40, no. 5, p. 80.

Crone, A.J., Machette, M.N., Bradley, L., and Mahan, S.A. 1997, Late Quaternary surface faulting on the Cheraw Fault, southeastern Colorado: U.S. Geological Survey Geologic Investigations Map Map I-2591, 1 sheet.

Dart, R.L., Volpi, C.M., Central United States Earthquake, C., Association of, C.S.G., and Geological, S., 2010, Earthquakes in the central United States, 1699-2010: [Reston, Va.]; Denver, Colo., U.S. Geological Survey ; Denver Publishing Service.

Grün, R.,1991, Age Calculation software for Riso Laboratories.

Hildenbrand, T., and Ravat, D., 1997, Geophysical setting of the Wabash Valley fault system: Seismological Research Letters, v. 68, p. 567-585.

Holbrook, J., and Schumm, S.A., 1999, Geomorphic and sedimentary response of rivers to tectonic deformation: A brief review and critique of a tool for recognizing subtle epeirogenic deformation in modern and ancient settings: Tectonophysics, v. 305, p. 287–306.

Jain, M. and Singhvi, A.K., 2001,Limits to depletion of blue-green light stimulated luminescence in feldspars: implications for quartz dating: Radiation Measurements, vol. 33, p. 883-892.

Kelson, K.I., Simpson, G.D., Haraden, C.C, Letttis, W.R., and Van Arsdale, R.B., 1994, Multiple late Holocene earthquakes along the Reelfoot Fault, central New Madrid Seismic Zone: National Earthquake Hazards Reduction Program final technical report for award number 1423-93-G-2293, 55 p.

Kent, G.M., Babcock, J.M., Driscoll, N.W., Harding, A.J., Dingler, J.A., Seitz, G.G., Gardner, J.V., Mayer, L.A., Goldman, C.R., Heyvaert, A.C., Richards, R.C., Karlin, R., Morgan, C.W., Gayes, P.T., and Owen, L.A., 2005, A 60 k.y. record of extension across the western boundary of the Basin and Range Province: Estimate slip rates from offset shoeline terraces and a catastrophic slide beneath Lake Tahoe. Geology, v. 33, p. 365–368.

Kim, W.-Y., 2003, The 18 June 2002 Caborn, Indiana, Earthquake: Reactivation of Ancient Rift in the Wabash Valley Seismic Zone?: Bulletin of the Seismological Society of America, v. 93, p. 2201-2211.

Li, Q., 2005, Stress evolution following the 1811–1812 large earthquakes in the New Madrid Seismic Zone: Geophysical Research Letters, v. 32, p. L11310.

Li, Q., Liu, M., Zhang, Q., and Sandvol, E., 2007, Stress evolution and seismicity in the central-eastern United States: Insights from geodynamic modeling, in Stein, S., and Mazzotti, S., ed., Continental Intraplate Earthquakes: Science, Hazard, and Policy Issues: Geological Society of America Special Paper

425, doi: 10.1130/2007.2425(11).

Mitchell, B., Nuttli, O., Herrmann, R., and Stauder, W., 1991, Seismotectonics of the central United States, in D.B. Slemmons, E.R.E., M.D. Zoback and D.D. Blackwell, ed., Neotectonics of North America, Volume 1, p. 245–260.

Munson, P., Obermeier, S., Munson, C., and Hajic, E., 1997, Liquefaction evidence for Holocene and latest Pleistocene seismicity in the southern halves of Indiana and Illinois: A preliminary overview: Seismological Research Letters, v. 68, p. 521-536.

Munson, P.J., and Munson, C.A., 1996, Paleoliquefaction evidence for recurrent strong earthquakes since 20,000 years BP in the Wabash Valley area of Indiana: Bloomington, Indiana University Department of Anthropology.

Murray, A.S., and Olley, J.M., 2002, Precision and accuracy in the optically stimulated luminescence dating of sedimentary quartz: a status review: Geochronometria, vol. 21, p. 11-16.

Murray, A.S., and Wintle, A.G., 2000, Luminescence dating of quartz using an improved single-aliquot regenerative-dose protocol: Radiation Measurements, v. 32, p. 57–73.

Murray, A.S., and Wintle, A.G., 2000, Application of the single-aliquot regenerative-dose protocol to the 375oC quartz TL signal: Radiation Measurements, vol. 32, p. 579-583.

Nelson, J.W., 1991, Sructural Styles of the Illinois Basin, in Leighton, M.W., Kolata, D.R., Oltz, D.F., and Eidel, J.J, ed., Interior Cratonic Basins, Volume 1, AAPG, p. 209-243.

Nuttli, O., and Zollweg, J., 1974, The relation between felt area and magnitude for central United States earthquakes: Bulletin of the Seismological Society of America, v. 64, p. 73.

Nuttli, O.W., 1979, Seismicity of the central United States: Rev. Eng. Geol.; (United States); v. 4, p. Pages: 67-94.

Obermeier, S., Bleuer, N., Munson, C., Munson, P., Martin, W., McWilliams, K., Tabaczynski, D., Odum, J., Rubin, M., and Eggert, D., 1991, Evidence of Strong Earthquake Shaking in the Lower Wabash Valley from Prehistoric Liquefaction Features: Science (New York, NY), v. 251, p.

Obermeier, S.F., 1993, Liquefaction evidence for one or more strong Holocene earthquakes in the Wabash Valley of southern Indiana and Illinois, with a preliminary estimate of magnitude: Washington, U.S. G.P.O.

Obermeier, S.F., 1996, Use of liquefaction-induced features for paleoseismic analysis - An overview of how seismic liquefaction features can be distinguished from other features and how their regional distribution and properties of source sediment can be used to infer the location and strength of Holocene paleoearthquakes: Engineering Geology, v. 44, p. 1-76.

Obermeier, S.F., 1998, Liquefaction evidence for strong earthquakes of Holocene and latest Pleistocene ages in the states of Indiana and Illinois, USA: Engineering Geology, v. 50, p. 227-254.

Obermeier, S.F., 2009, Using liquefaction-induced and other soft-sediment features for paleoseismic analysis in McCalpin, J.P., ed., Paleoseismology: International Geophysics, v. 95, p. 497-564.

Olson, S.M., Green, R.A., and Obermeier, S.F., 2005, Revised magnitude-bound relation for the Wabash

Valley Seismic Zone of the central United States: Seismological Research Letters, v. 76, no. 4, p. 756–771.

Porat, N., 2006, Use of magnetic separation for purifying quartz for luminescence dating: Ancient TL, vol. 24, p.33-36.

Prescott, J.R., and Hutton, J.T., 1994, Cosmic ray contributions to dose rates for luminescence and ESR dating: Large depths and long-term time variations: Radiation Measurements, vol. 23, p. 497-500.

Reiter, L, 1995, Paleoseismology-A users Perspective in Perspectives in Paleoseismology, Assoc. of Engineering Geologists Special Publication 6, p. 3-6.

René, R.M., and Stanonis, F.L., 1995, Reflection seismic profiling of the Wabash Valley fault system in the Illinois Basin: U.S. Geological Survey Professional Paper 1538-Ohio River, 33 p.

Rutledge, F.A., 2004, High resolution geophysical investigation of late quaternary deformation in the lower Wabash valley fault system: M.S. Thesis, Lexington, Ky., [University of Kentucky Libraries].

Schumm, S.A., 1985, Patterns of Alluvial Rivers: Annual Review of Earth and Planetary Sciences, v. 13, p. 5-27.

Schumm, S.A., Dumont, J F, and Holbrook, J M, 2000, Active Tectonics and Alluvial Rivers, Cambridge University Press, 276 p.

Sexton, J., Braile, L., Hinze, W., and Campbell, M., 1986, Seismic reflection profiling studies of a buried Precambrian rift beneath the Wabash Valley fault zone: Geophysics, v. 51, p. 640-660.

Taylor, K.B., R. B. Herrmann, M. W. Hamburger, G. L. Pavlis, A. Johnston, C. J. Langer, and C. Lam, 1989, The southeastern Illinois earthquake of 10 June 1987: Seismological Research Letters, v. 60, p. 101-110.

Rhea, S., and Wheeler, R.L., 1996, Map showing seismicity in the vicinity of the lower Wabash Valley, Illinois, Indiana, and Kentucky: U.S. Geological Survey Miscellaneous Investigations Report I-2583-A, , plus 14 p.

Singhvi, A.K, and Porat, N., 2008, Impact of luminescence dating on geomorphological and palaeoclimate research in drylands: Boreas, vol. 37, p. 536-558.

Suzuki, K., Toda, S., Kusunoki, K., Fujimitsu, Y., Mogi, T., and Jomori, A., 2000, Case studies of electrical and electromagnetic methods applied to mapping active faults beneath the thick quaternary, in Yuji Kanaori, K. T., and Masahiro, C., eds., Developments in Geotechnical Engineering, Volume Volume 84, Elsevier, p. 29-45.

Van Arsdale, R., Counts, R., and Woolery, E, 2009, Quaternary Displacement Along the Hovey Lake Fault of Southern Indiana, U.S. Geological Survey- National Earthquake Hazards Reduction Program Final Technical Report. Award 07HQGR0052, 11p.

Wheeler, R.L., Rhea, Susan, Diehl, S.F., Drahovzal, J.A., Bear, G.W., and Sargent, M.L., 1997, Seismotectonic map showing faults, igneous rocks, and geophysical and neotectonic features in the vicinity of the lower Wabash Valley, Illinois, Indiana, and Kentucky: U.S. Geological Survey Geologic Investigations Series Map I-2583-D, 1 sheet, scale 1:250,000, 19 p. pamphlet.

Appendix A

Core Descriptions

Borehole	11-001b						
Latitude:	37.859436°						
Longitud	-87.893988°						
Drive #	Interval (meters)	From (meters)	To (meters)	Lithology	Munsell	Color	Comments
1	0 — 1.25	0	-0.29	silty clay loam	10YR 3/3	dark brown	many roots and organics, weak subangular blocky to granular structure
1	0 — 1.25	-0.29	-0.39	silt loam	10YR 4/2	dark grayish brown	many roots and organics, subangular blocky structure
1	0 — 1.25	-0.39	-1.24	silty clay loam	10YR 4/4	dark yellowish brown	few to common roots, prismatic and SBK structure
2	1.25 — 2.5	-1.25	-1.75	silty clay loam	10YR 4/4	dark yellowish brown	few Mn stains, 2SBK structure
2	1.25 — 2.5	-1.75	-1.98	silty clay loam	10YR 4/4	dark yellowish brown	many 7.5 YR 5/6 Mn stains and accumulations
2	1.25 — 2.5	-1.98	-2.5	silty clay loam	10YR 4/4	dark yellowish brown	many Mn and Fe stains
3	2.5 — 3.75	-2.5	-2.7	loam	10YR 4/4	dark yellowish brown	loam to sandy loam, few Mn stains
3	2.5 — 3.75	-2.7	-3.46	sandy loam	10YR 4/4	dark yellowish brown	sandy loam, few Mn stains
3	2.5 — 3.75	-3.46	-3.75	loamy sand	10YR 4/4	dark yellowish brown	loamy fine sand, Mn-Fe stains common
4	3.75 — 5	-3.75	-3.83	clay loam	5Y 4/1	dark gray	thin clay bed
4	3.75 — 5	-3.83	-4.61	loamy sand	10YR 4/4	dark yellowish brown	loamy fine sand to a fine sand, massive and well sorted
4	3.75 — 5	-4.61	-4.95	loamy sand	10YR 4/4	dark yellowish brown	loamy fine sand with clay loam laminations
5	5 — 6.25	-5	-5	interval is missing	0	interval is missing	interval is missing
6	6.25 — 7.5	-6.25	-7.5	clay	2.5Y 4/2	dark grayish brown	clay to clay loam with a few fine sand beds throughout
7	7.5 — 8.75	-7.5	-8.25	clay	5Y 4/1	dark gray	clay with fine sand beds throughout interval
7	7.5 — 8.75	-8.25	-8.6	sandy clay	10YR 4/4	dark yellowish brown	sandy clay wih fine sand laminae; Paleosol?
7	7.5 — 8.75	-8.6	-8.75	coarse sand	10YR 5/4	yellowish brown	coarse to medium, poorly-sorted sand
8	8.75 — 9.75	-8.75	-9.75	coarse sand	10YR 5/4	yellowish brown	coarse, poorly-sorted sand

Borehole id:11-002
Latitude: 37.859435°
Longitude: -87.894046°

Drive #	Interval (meters)	From (meters)	To (meters)	Lithology	Munsell	Color	Comments
1	0 — 1.25	0	-0.28	silty clay loam	10YR 4/2	dark grayish brown	many roots, very weak granular structure to structureless Ap (plow zone?)
1	0 — 1.25	-0.28	-1.12	silty clay loam	10YR 3/3	dark brown	few Mn stains, some fine organic flecks throughout
2	1.25 — 2.5	-1.25	-1.49	silty clay loam	10YR 3/3	dark brown	cutting shoe plugged, pushed through lower interval without coring (nailed through)
2	1.25 — 2.5	-1.49	-2.5	LOST	LOST	LOST	LOST
3	2.5 — 3.75	-2.5	-2.6	clay loam	10YR 4/3	brown	light clay, borderline silty clay loam
3	2.5 — 3.75	-2.6	-2.8	loamy sand	10YR 4/3	brown	
3	2.5 — 3.75	-2.8	-3.75	fine sand	10YR 4/3	brown	moderately sorted fine to medium sand
4	3.75 — 3.85	-3.75	-3.85	LOST	LOST	LOST	LOST, piston rode up before core interval reached; contaminated so interval was discarded
5	3.85 — 5	-3.85	-4.5	fine sand	10YR 4/3	brown	well sorted
5	3.85 — 5	-4.5	-4.6	medium sand	10YR 4/4	dark yellowish brown	well sorted, few Mn stains
5	3.85 — 5	-4.6	-5	sandy clay	10YR 4/3	brown	many Mn stains and fine concretions
6	5 — 6.25	-5	-5.1	sandy loam	10YR 4/2	dark grayish brown	
6	5 — 6.25	-5.1	-5.28	loam	2.5Y 4/2	dark grayish brown	interbedded sands and clay
6	5 — 6.25	-5.28	-5.7	clay loam	5Y 4/1	dark gray	few mm scale fine sand laminae
6	5 — 6.25	-5.7	-6.05	clay loam	5Y 4/1	dark gray	mm scale fine sand laminae throughout interval
7	6.25 — 7.5	-6.25	-6.33	clay loam	5Y 4/1	dark gray	mm scale fine sand laminae throughout interval
7	6.25 — 7.5	-6.33	-6.42	heavy clay loam	5Y 4/1	dark gray	
7	6.25 — 7.5	-6.42	-6.6	clay loam	5Y 4/1	dark gray	mm scale fine sand laminae throughout interval
7	6.25 — 7.5	-6.6	-7	clay loam	5Y 4/1	dark gray	mm scale fine sand laminae throughout interval
7	6.25 — 7.5	-7	-7.35	clay loam	5Y 4/1	dark gray	mm scale fine sand laminae throughout interval
8	7.5 — 8.75	-7.5	-8.75	coarse sand	10YR 5/4	yellowish brown	moderately sorted
9	8.75 — 10	-8.75	-10	coarse sand	10YR 5/4	yellowish brown	moderately sorted
10	10 — 10.72	-10	-10.5	coarse sand	10YR 5/4	yellowish brown	moderately sorted
10	10 — 10.72	-10.5	-10.72	coarse sand	10YR 5/4	yellowish brown	poorly sorted pebble sand. Refusal on pebble sand

Borehole id: 11-003							
Latitude: 37.859436°							
Longitude: -87.894107°							
Drive #	Interval (meters)	From (meters)	To (meters)	Lithology	Munsell	Color	Comments
1	0 — 1.25	0	-0.12	silty clay loam	10YR 4/2	dark grayish brown	many roots, single grain (structureless, Ap plow zone)
1	0 — 1.25	-0.12	-0.96	silty clay loam	10YR 4/2	dark grayish brown	rare Mn stains
2	1.25 — 2.5	-1.25	-1.84	silty clay loam	10YR 4/3	brown	massive (no structure), few Mn stains
2	1.25 — 2.5	-1.84	-2.3	loamy sand	10YR 4/3	brown	
2	1.25 — 2.5	-2.3	-2.5	medium sand	10YR 4/4	dark yellowish brown	moderately sorted
3	2.5 — 3.75	-2.5	-2.95	medium sand	10YR 4/4	dark yellowish brown	moderately sorted
3	2.5 — 3.75	-2.95	-3.28	loamy sand	10YR 4/4	dark yellowish brown	common Mn stins and redoximorphic coloring
3	2.5 — 3.75	-3.28	-3.7	fine sand	10YR 4/4	dark yellowish brown	well sorted
4	3.75 — 5	-3.75	-4.24	fine sand	10YR 4/4	dark yellowish brown	well sorted
4	3.75 — 5	-4.24	-4.31	loamy sand	10YR 3/3	dark brown	many Mn stains and concretions
4	3.75 — 5	-4.31	-4.55	silty clay loam	10YR 4/3	brown	Mn concretions common
4	3.75 — 5	-4.55	-4.67	sandy loam	2.5Y 4/3	olive brown	
4	3.75 — 5	-4.67	-4.9	silty clay loam	2.5Y 4/3	olive brown	
5	5 — 6.25	-5	-5.08	fine sand	10YR 4/3	brown	
5	5 — 6.25	-5.08	-6.18	clay loam	2.5Y 4/1	dark gray	few mm scale fine sand laminae
6	6.25 — 7.5	-6.25	-7.3	clay loam	5Y 4/1	dark gray	cm scale fine sand beds throughout interval
6	6.25 — 7.5	-7.3	-7.4	loam	10YR 4/6	dark yellowish brown	many Mn concretions; PALEOSOL
7	7.5 — 8.75	-7.5	-7.72	medium sand	10YR 4/4	dark yellowish brown	moderately sorted
7	7.5 — 8.75	-7.94	-8.3	coarse sand	10YR 5/6	yellowish brown	moderately sorted coarse to medium sand
7	7.5 — 8.75	-8.3	-8.7	coarse sand	10YR 5/6	yellowish brown	poorly sorted coarse sand with pebbles
8	9 — 10	-9	-10	coarse sand	10YR 5/6	yellowish brown	poorly sorted coarse sand with pebbles
9	10 — 11	-10	-10.85	coarse sand	10YR 5/6	yellowish brown	poorly sorted coarse to very coarse sand with pebbles
9	10 — 11	-10.85	-11	coarse pebble sand	10YR 5/6	yellowish brown	poorly sorted coarse pebble sand to sandy pebble gravel.
10	11 — 12.25	-11	-12.25	medium sand	2.5Y 5/3	light olive brown	moderately sorted
11	12.25 - 13.5	-12.25	-12.89	medium sand	2.5Y 5/3	light olive brown	moderately sorted
11	12.25 - 13.5	-12.89	-13.5	coarse pebble sand	2.5Y 5/3	light olive brown	coarsening downward poorly sorted coarse pebble sand

Borehole id: 11-004							
Latitude: 37.859439°							
Longitude: -87.894169°							
Drive #	Interval (meters)	From (meters)	To (meters)	Lithology	Munsell	Color	Comments
1	0 — 1.25	0	-0.32	silt loam	10YR 3/2	very dark grayish brown	many roots and organics, weak subangular blocky structure
1	0 — 1.25	-0.32	-0.95	silty clay loam	10 YR 4/3	brown	common Mn stains, burrows, very weak 1SBK structure (weak subangular blocky)
2	1.25 — 2.5	-1.25	-1.45	silty clay loam	10 YR 4/3	brown	massive to granular (almost structureless!?) few Mn stains
2	1.25 — 2.5	-1.45	-1.56	clay loam	10 YR 4/3	brown	clay loam to silty clay loam, micaceous
2	1.25 — 2.5	-1.56	-1.75	loam	10 YR 4/3	brown	
2	1.25 — 2.5	-1.75	-2.35	medium sand	10 YR 4/3	brown	moderately sorted medium sand
3	2.5 — 3.75	-2.5	-2.65	medium sand	2.5Y 4/3	olive brown	moderately to poorly sorted medium to fine sand
3	2.5 — 3.75	-2.65	-2.8	silty clay	5Y 4/2	olive gray	
3	2.5 — 3.75	-2.8	-3.75	fine sand	2.5Y 4/3	olive brown	well sorted fine sand
4	3.75 — 5	-3.75	-4	fine sand	10YR 4/3	brown	well sorted fine sand, Mn stains common
4	3.75 — 5	-4	-4.33	loam	10YR 4/3	brown	few Mn stains
4	3.75 — 5	-4.33	-4.42	sandy loam	10YR 4/3	brown	
4	3.75 — 5	-4.42	-4.47	fine sand	10YR 4/3	brown	
4	3.75 — 5	-4.47	-4.85	clay	5Y 4/2	olive gray	clay to silty clay, massive
5	5 — 6.25	-5	-5.97	clay	5Y 4/1	dark gray	clay to clay loam with fine sand laminae throughout interval
5	5 — 6.25	-5.97	-5.99	medium sand	10YR 4/4	dark yellowish brown	sharp contact
6	6.25 — 7.5	-6.25	-6.82	clay loam	5Y 4/1	dark gray	clay to clay loam with fine sand laminae throughout interval
6	6.25 — 7.5	-6.82	-7.16	silt loam	10YR 4/4	dark yellowish brown	many sand laminae, many Mn stains
6	6.25 — 7.5	-7.16	-7.2	medium sand	10YR 4/4	dark yellowish brown	well sorted
7	7.5 — 8.25	-7.5	-8.35	medium sand	10YR 4/3	brown	moderately sorted medium sand
7	7.5 — 8.25	-8.35	-8.7	fine sand	5Y 4/1	dark gray	
7	7.5 — 8.25	-8.7	-8.75	clay	5Y 4/1	dark gray	
8	8.25 — 9.9	-8.25	-9.9	coarse sand	2.5Y 4/3	olive brown	coarse pebble sand, poorly sorted
9	10 — 11.12	-10	-10.6	medium sand	2.5Y 4/2	dark grayish brown	moderately to poorly sorted medium sand
9	10 — 11.12	-10.6	-10.8	coarse sand	2.5Y 4/2	dark grayish brown	coarse pebble sand, poorly sorted
9	10 — 11.12	-10.8	-11.15	sandy gravel	2.5Y 4/2	dark grayish brown	poorly sorted sandy pebble gravel. Refusal on gravel

Borehole id: 12-002							
Latitude: 37.859436°							
Longitude: -87.894222°							
Drive #	Interval (meters)	From (meters)	To (meters)	Lithology	Munsell	Color	Comments
1	0 — 1.5	0	-0.3	silt loam	10 YR 4/3	brown	silt loam to silty clay loam, weak fine subangular blocky structure, many roots
1	0 — 1.5	-0.3	-0.86	silt loam	10 YR 4/3	brown	silt loam to silty clay loam, very weak fine subangular blocky structure, many roots
1	0 — 1.5	-0.86	-1.48	silty clay loam	10 YR 4/3	brown	fine subangulat blocky structure, better developed than previous interval
2	1.5 — 3	-1.5	-1.69	silt loam	10YR 4/4	dark yellowish brown	mica flakes visible, no acid reaction
2	1.5 — 3	-1.69	-2	sandy clay loam	10YR 4/3	brown	
2	1.5 — 3	-2	-2.1	loamy sand	10YR 4/3	brown	
2	1.5 — 3	-2.1	-2.9	fine sand	10YR 4/4	dark yellowish brown	
3	3 — 4.42	-3	-3.19	fine to med sand	10YR 4/4	dark yellowish brown	
3	3 — 4.42	-3.19	-3.25	loamy sand	10YR 4/4	dark yellowish brown	few Mn concretions
3	3 — 4.42	-3.25	-3.3	sandy loam	10YR 5/2	grayish brown	
3	3 — 4.42	-3.3	-3.44	fine to med sand	10YR 4/4	dark yellowish brown	
3	3 — 4.42	-3.44	-3.62	silt loam	10YR 4/3	brown	many Mn concretions from -3.48 -3.62 interval
3	3 — 4.42	-3.62	-3.72	sandy loam	10YR 4/3	brown	
3	3 — 4.42	-3.72	-3.8	loamy sand	10YR 4/3	brown	
3	3 — 4.42	-3.8	-3.92	medium sand	10YR 4/4	dark yellowish brown	moderately sorted
3	3 — 4.42	-3.92	-3.99	sandy clay	10YR 5/3	brown	
3	3 — 4.42	-3.99	-4.05	medium sand	10YR 3/4	dark yellowish brown	moderately sorted
4	4.5 — 5.82	-4.5	-4.62	medium sand	10YR 4/4	dark yellowish brown	well sorted
4	4.5 — 5.82	-4.62	-4.63	silty clay	2.5Y 5/2	grayish brown	
4	4.5 — 5.82	-4.63	-4.64	medium sand	10YR 4/4	dark yellowish brown	well sorted
4	4.5 — 5.82	-4.64	-4.65	fine sand	10YR 4/4	dark yellowish brown	well sorted
4	4.5 — 5.82	-4.65	-4.94	clay	5Y 4/1	dark gray	massive
4	4.5 — 5.82	-4.94	-5.12	clay loam	5Y 4/1	dark gray	
4	4.5 — 5.82	-5.12	-5.22	clay	5Y 4/1	dark gray	
4	4.5 — 5.82	-5.22	-5.3	clay loam	5Y 4/1	dark gray	
4	4.5 — 5.82	-5.3	-5.4	clay loam	5Y 4/1	dark gray	fine sand laminae through interval
4	4.5 — 5.82	-5.4	-5.45	loamy sand	5Y 4/2	olive gray	
4	4.5 — 5.82	-5.45	-5.51	clay loam	5Y 4/1	dark gray	
4	4.5 — 5.82	-5.51	-5.7	silty clay loam	5Y 4/1	dark gray	
5	5.82 — 7	-5.82	-5.88	fine sand	5Y 4/2	olive gray	
5	5.82 — 7	-5.88	-6.01	silty clay loam	5Y 4/1	dark gray	fine sand laminae throughout interval
5	5.82 — 7	-6.01	-6.39	clay	5Y 4/1	dark gray	fine sand laminae and a few fine organics throughout interval
5	5.82 — 7	-6.39	-6.52	silty clay loam	5Y 4/1	dark gray	fine sand laminae and a few fine organics throughout interval, (2.5y 4/3 olive brown) at base of interval
5	5.82 — 7	-6.52	-6.62	silty clay loam	2.5Y 4/3	olive brown	many Mn stains
5	5.82 — 7	-6.62	-6.8	medium sand	7.5YR 4/4	brown	many Mn stains and concretions
6	7 — 8.25	-7	-7.8	medium sand	2.5 Y 4/4	olive brown	moderately sorted
6	7 — 8.25	-7.8	-8.25	coarse sand	2.5 Y 4/4	olive brown	moderately to poorly sorted
7	8.25 — 9	-8.25	-8.9	coarse sand	2.5 Y 4/4	olive brown	poorly sorted
7	8.25 — 9	-8.9	-9	sandy pebble gravel	2.5 Y 4/4	olive brown	poorly sorted

Borehole id:12-003							
Latitude:	37.859431°						
Longitud	-87.894307°						
Drive #	Interval (meters)	From (meters)	To (meters)	Lithology	Munsell	Color	Comments
1	0 — 1.5	0	-0.25	silty clay loam	10YR 4/2	dark grayish brown	few fine Mn stains, weak subangular blocky structure, many roots
1	0 — 1.5	-0.25	-1.25	silty clay loam	10YR 4/3	brown	few fine Mn concretions
2	1.5 — 3	-1.5	-1.58	clay	2.5Y 4/2	dark grayish brown	
2	1.5 — 3	-1.58	-1.87	sandy clay	2.5Y 4/2	dark grayish brown	has 7.5 YR 4/6 Fe stains and is slightly mottled
2	1.5 — 3	-1.87	-2.13	sandy loam	10YR 4/4	dark yellowish brown	mottled with 2.5Y 4/2 reduced zones
2	1.5 — 3	-2.13	-2.26	loamy sand	10YR 4/4	dark yellowish brown	
2	1.5 — 3	-2.26	-2.42	silty clay	2.5Y 4/2	dark grayish brown	few organics
2	1.5 — 3	-2.42	-2.61	silty clay	2.5Y 4/2	dark grayish brown	bioturbated, PALEOSOL
3	3 — 4.5	-3	-3.5	silty clay loam	10YR 4/2	dark grayish brown	burrows, orgaincs, few Mn stains
3	3 — 4.5	-3.5	-3.65	silty clay loam	2.5Y 4/2	dark grayish brown	burrows, orgaincs, few Mn stains
3	3 — 4.5	-3.65	-3.98	silty clay loam	2.5Y 4/2	dark grayish brown	
3	3 — 4.5	-3.98	-4.18	silty clay loam	2.5Y 4/2	dark grayish brown	Mn stains common
4	4.5 — 5.25	-4.5	-4.84	clay	5Y 4/1	dark gray	
4	4.5 — 5.25	-4.84	-4.92	fine sand	5Y 4/3	olie	moderately to well sorted micaceous sand
4	4.5 — 5.25	-4.92	-5.54	clay	5Y 4/1	dark gray	interval has a 2 cm thick olive (5Y 4/3) fine sand sand bed @-5.22 m
5	5.75 — 7	-5.75	-6.19	clay	5Y 4/1	dark gray	interbedded clay and mm scale fine sand beds throughout interval
0	5.75 — 7	-6.19	-6.3	clay loam	5Y 4/1	dark gray	interbedded clay and mm scale fine sand beds throughout interval
0	5.75 — 7	-6.3	-6.58	loam	10YR 4/3	brown	mottled, has sand laminae, Mn stains common, PALEOSOL?
0	5.75 — 7	-6.58	-6.89	medium sand	10YR 4/4	dark yellowish brown	moderately sorted
6	7 — 8.25	-7	-8.25	medium sand	10YR 4/4	dark yellowish brown	moderately sorted
7	8.25 — 9	-8.25	-9	medium sand	10YR 4/4	dark yellowish brown	moderately sorted
8	9 — 10	-9	-10	coarse sand	10YR 4/4	dark yellowish brown	moderately sorted

Borehole id: 12-004
Latitude: 37.859443° Longitude: -87.894455

Drive #	Interval (meters)	From (meters)	To (meters)	Lithology	Munsell	Color	Comments
1	0.0 — 0.91	0	-0.15	Silt loam	10YR 4/2	very dark grayish brown	weak subangular blocky structure, many roots
1	0.0 — 0.91	-0.15	-0.64	Silt loam	2.5Y 3/1	very dark gray	weak subangular blocky structure, many roots
1	0.0 — 0.91	-0.64	-0.91	silty clay loam	2.5Y 3/1	very dark gray	granular structure, laminae of coarser silt throughtout interval
2	0.91 — 1.83	-0.91	-1.18	silty clay	2.5Y 4/3	olive brown	wood fragment at -1.18 m (root)
2	0.91 — 1.83	-1.18	-1.65	silty clay	2.5Y 4/3	olive brown	many Mn stains
3	1.83 — 2.74	-1.83	-1.96	silty clay	2.5Y 4/3	olive brown	
3	1.83 — 2.74	-1.96	-2.56	clay	2.5Y 4/3	olive brown	many Mn-Fe stains and concretions
3	1.83 — 2.74	-1.96	-2.05	clay	5Y 4/2	olive gray	very few Mn stains
3	1.83 — 2.74	-2.05	-2.14	clay	2.5Y 4/2	dark grayish brown	few to common Mn and Fe stains and small concretions
4	2.74 — 3.66	-2.74	-2.83	clay	2.5Y 4/3	olive brown	massive, no Mn or FE stains
4	2.74 — 3.66	-2.83	-3.14	silty clay	2.5Y 4/3	olive brown	few Mn stains
4	2.74 — 3.66	-3.14	-3.56	clay	5Y 4/2	olive gray	few Mn stains, massive, roots from -.3.4 to -3.14 m; paleosol?
5	3.66 — 4.57	-3.66	-3.95	silty clay	2.5Y 4/3	olive brown	
5	3.66 — 4.57	-3.95	-4.12	clay	5Y 4/2	olive gray	some organic flecks
5	3.66 — 4.57	-4.12	-4.28	silty clay loam	2.5Y 4/3	olive brown	few Mn stains
6	4.57 — 5.49	-4.57	-4.69	clay	5Y 4/2	olive gray	
6	4.57 — 5.49	-4.69	-4.98	clay loam	2.5Y 4/3	olive brown	few Mn stains
6	4.57 — 5.49	-4.98	-5.4	sandy clay loam	5Y 4/3	olive	
7	5.49 — 6.4	-5.49	-5.77	sandy loam	2.5Y 4/3	olive brown	
7	5.49 — 6.4	-5.77	-5.94	sandy loam	2.5Y 4/3	olive brown	
7	5.49 — 6.4	-5.94	-5.98	loam	2.5Y 4/3	olive brown	Mn stains common
7	5.49 — 6.4	-5.98	-6.02	loam	2.5Y 4/3	olive brown	Mn stains common
7	5.49 — 6.4	-6.02	-6.09	clay loam	2.5Y 4/3	olive brown	Mn stains common
7	5.49 — 6.4	-6.09	-6.12	loamy sand	2.5Y 4/3	olive brown	
7	5.49 — 6.4	-6.12	-6.16	clay loam	2.5Y 4/3	olive brown	Mn concretions
7	5.49 — 6.4	-6.16	-6.36	sandy clay loam	2.5Y 4/3	olive brown	
8	6.4 — 7.32	-6.4	-6.8	loamy sand	2.5Y 4/3	olive brown	clay laminae at -6.62 and -6.70 m
8	6.4 — 7.32	-6.8	-7.12	loamy sand	2.5Y 4/2	dark grayish brown	clay laminae at-7.86 and -7.02 m
8	6.4 — 7.32	-7.12	-7.33	sand	10Y 4/1	dark greenish gray	moderately sorted fine- to medium sand
9	7.32 —8.23	-7.32	-7.37	sandy loam	10Y 4/1	dark greenish gray	sandy loam with very fine clay laminae2.5Y 4/3
9	7.32 —8.23	-7.37	-7.38	clay	5Y 4/1	dark gray	
9	7.32 —8.23	-7.38	-7.42	sandy loam	10YR 4/1	dark greenish gray	sandy loam with very fine clay laminae
9	7.32 —8.23	-7.42	-7.55	sandy loam	5Y 4/1	dark gray	fine sandy loam (medium sand)
9	7.32 —8.23	-7.55	-7.68	sand	5Y 4/1	dark gray	well sorted fine sand
9	7.32 —8.23	-7.68	-7.87	sand	5Y 4/1	dark gray	interbedded 5Y 4/1 fine sand and clay
9	7.32 —8.23	-7.87	-7.96	loamy sand	5Y 4/1	dark gray	loamy sand; organics at -7.91
9	7.32 —8.23	-7.96	-8.05	clay loam	10YR 3/1	very dark gray	
9	7.32 —8.23	-8.05	-8.11	sand	10YR 3/1	very dark gray	
10	8.23 — 9.14	-8.23	-9.05	sand	10YR 3/1	very dark gray	moderately sorted , medium to fine sand with clay laminae at -8.26, -8.30, -8.38, -8.56 to -8.60, -8.76, -8.99 to -9.01
11	8.23 — 9.14	-9.14	-9.28	sandy clay	10YR 3/1	very dark gray	
11	8.23 — 9.14	-9.28	-9.36	sand	5Y 4/1	dark gray	poorly sorted fine to medium sand
11	8.23 — 9.14	-9.36	-9.66	sand	2.5Y 4/3	olive brown	poorly sorted, coarse pebble sand to fine sandy pebble gravel

Borehole id:12-005							
Latitude:	37.859436°						
Longitud	-87.893988°						
Drive #	Interval (meters)	From (meters)	To (meters)	Lithology	Munsell	Color	Comments
1	0 — 1	0	-0.18	silty clay loam	10YR 4/2	dark grayish brown	many roots and organics, very weak subangular blocky structure (1SBK)
1	0 — 1	-0.18	-0.3	silty clay loam	10YR 4/2	dark grayish brown	granular structure, few Mn stains
1	0 — 1	-0.3	-0.9	silty clay loam	10YR 4/3	brown	Mn stains common
2	1 — 1.91	-1	-1.91	silty clay loam	10YR 4/3	brown	reoximorphic colors, burrows, many Mn stains (PALEOSOL?)
3	1.91 — 2.83	-1.91	-2.11	silty clay loam	10YR 4/3	brown	burrow filled with 2.5Y 4/3 clay
3	1.91 — 2.83	-2.11	-2.52	light clay loam	10YR 4/3	brown	few Mn stains
3	1.91 — 2.83	-2.52	-2.83	sandy clay loam	10YR 4/3	brown	
4	2.83 — 3.74	-2.83	-3.74	LOST	LOST	LOST	LOST
5	3.74 — 4.65	-3.74	-3.84	loamy fine sand	10YR 4/4	dark yellowish brown	
5	3.74 — 4.65	-3.84	-4.15	fine sand	10YR 4/4	dark yellowish brown	few Mn stains
5	3.74 — 4.65	-4.15	-4.49	coarse sand	10 YR 5/6	yellowish brown	moderately to well sorted
5	3.74 — 4.65	-4.49	-4.65	loamy sand	10YR 4/4	dark yellowish brown	

Borehole id:12-007							
Latitude:	37.859435°						
Longitud	-87.893930°						
Drive #	Interval (meters)	From (meters)	To (meters)	Lithology	Munsell	Color	Comments
1	0 — 1.4	0	-0.3	silt loam	10YR 4/2	dark grayish brown	many roots, single grain to structureless, plow zone
1	0 — 1.4	-0.3	-1.25	silty clay loam	10YR 4/3	brown	many roots and organic matter, 1SBK structure
2	1.4 — 2.75	-1.4	-1.77	silty clay loam	10YR 4/3	brown	few Mn stains
2	1.4 — 2.75	-2.8	-4.15	silty clay loam	10YR 4/3	brown	MN concretions and stains common
2	1.4 — 2.75	-2.8	-4.15	silty clay loam	10YR 4/3	brown	few Mn stains
2	1.4 — 2.75	-2.2	-2.55	light clay loam	10YR 4/3	brown	Mn stains rare
3	2.75 — 4	-2.75	-3.55	loam	10YR 4/3	brown	
3	2.75 — 4	-3.55	-3.95	sandy loam	10YR 4/3	brown	
4	4 — 5.25	-4	-4.33	loamy sand	10YR 4/3	brown	
4	4 — 5.25	-4.33	-4.8	fine sand	10YR 4/3	brown	
4	4 — 5.25	-4.8	-5.25	loamy fine sand	10YR 4/3	brown	
5	5.35 — 6.75	-5.35	-6.15	silty clay	2.5Y 4/2	dark grayish brown	few fine sand laminae
5	5.35 — 6.75	-6.15	-6.64	clay loam	2.5Y 4/2	dark grayish brown	laminated with mm scale fine sand throughout interval
6	6.75 — 8.15	-6.75	-7.75	clay loam	5Y 4/1	dark gray	laminated with mm scale fine sand throughout interval
6	6.75 — 8.15	-7.75	-8.1	clay loam	10YR 4/6	dark yellowish brown	laminated with mm scale fine sand throughout interval, burrowed? and Mn concretions (PALEOSOL)
7	8.15 — 9.5	-8.15	-8.33	medium sand	10YR 4/4	dark yellowish brown	well sorted medium sand
7	8.15 — 9.5	-8.33	-8.38	clay loam	2.5Y 4/3	olive brown	
7	8.15 — 9.5	-8.38	-9.29	coarse sand	10YR 4/4	dark yellowish brown	moderately sorted, refusal on coarse sand